



# Zirconia- and ceria-based electrolytes for fuel cell applications: critical advancements toward sustainable and clean energy production

Tushar Kanti Maiti<sup>1</sup> · Jagannath Majhi<sup>1</sup> · Subrata Kumar Maiti<sup>1</sup> · Jitendra Singh<sup>1</sup> · Prakhar Dixit<sup>1</sup> · Tushita Rohilla<sup>2</sup> · Samaresh Ghosh<sup>1</sup> · Sakchi Bhushan<sup>3</sup> · Sujay Chattopadhyay<sup>1</sup>

Received: 11 June 2022 / Accepted: 14 July 2022 / Published online: 21 July 2022  
© The Author(s), under exclusive licence to Springer-Verlag GmbH Germany, part of Springer Nature 2022

## Abstract

Solid oxide fuel cells (SOFCs) are emerging as energy conversion devices for large-scale electrical power generation because of their high energy conversion efficiency, excellent ability to minimize air pollution, and high fuel flexibility. In this context, this critical review has focussed on the recent advancements in developing a suitable electrolyte for SOFCs which has been required for the commercialization of SOFC technology after emphasizing the literature from the prior studies. In particular, the significant developments in the field of solid oxide electrolytes for SOFCs, particularly zirconia- and ceria-based electrolytes, have been highlighted as important advancements toward the production of sustainable and clean energy. It has been reported that among various electrolyte materials, zirconia-based electrolytes have the potential to be utilized as the electrolyte in SOFC because of their high thermal stability, non-reducing nature, and high mechanical strength, along with acceptable oxygen ion conductivity. However, some studies have proved that the zirconia-based electrolytes are not suitable for low and intermediate-temperature working conditions because of their poor ionic conductivity to below 850 °C. On the other hand, ceria-based electrolytes are being investigated at a rapid pace as electrolytes for intermediate and low-temperature SOFCs due to their higher oxygen ion conductivity with good electrode compatibility, especially at lower temperatures than stabilized zirconia. In addition, the most emerging advancements in electrolyte materials have demonstrated that the intermediate temperature SOFCs as next-generation energy conversion technology have great potential for innumerable prospective applications.

**Keywords** Fuel cells · Ceria · Zirconia · Clean energy · Sustainable materials · Electrolytes

## Introduction

Expanding economies largely depend on fossil fuels for the fulfillment of rising needs of energy for both transportation and stationary sectors. However, fossil fuels are non-renewable, and their availability is limited. Furthermore, burning fossil fuels releases greenhouse gases such as CO, CO<sub>2</sub>, SO<sub>x</sub>, and NO<sub>x</sub>, contributing to global warming

and air pollution. Furthermore, mining fossil fuels from the depths of the earth has a negative impact on the ecosystem. Therefore, it is essential to create clean, sustainable energy technologies to satisfy the enormous growth in global energy consumption (Wei and Li 2008; Li et al. 2014; Sacanell et al. 2017). The progress of multidisciplinary research is emerging faster because of increasing global connectivity, which will replace multiple materials and equipment that are being used recently. The future world would be a combination of advanced materials and new sustainable energy sources because it needs to protect the environment and human health and maintain the increasing demand for social, economic, and industrial needs (Hassen et al. 2016b; Morales et al. 2018; Hou et al. 2021). The demand for electrical energy is increasing because of the growing world population and rapid industrialization. The world energy demand is dependent mainly on fossil fuels, but various disadvantages related to fossil fuels like limited availability, greenhouse gas emissions, and environmental

Responsible Editor: George Z. Kyzas

✉ Sujay Chattopadhyay  
sujay@pe.iitr.ac.in

<sup>1</sup> Department of Polymer and Process Engineering, IIT Roorkee Saharanpur Campus, Saharanpur 247001, India

<sup>2</sup> Department of Mechanical Engineering, IIT Ropar, Punjab 140 001, India

<sup>3</sup> Department of Paper Technology, IIT Roorkee Saharanpur Campus, Saharanpur 247001, India

pollution divert the global energy research trend from fossil fuels to renewable energy sources. Expanding economies predominantly depend on fossil fuels that are mainly used to fulfil escalating demands of energy for both transportation and stationary sectors. However, fossil fuels are non-renewable, and their availability is limited. A few sustainable technologies, such as solar cells, wind power, tidal energy, and hydropower can be used to supply clean energy by utilizing renewable energy sources (Zhang et al. 2019; Jang et al. 2020; Ren et al. 2020a). Hence, the search for renewable and sustainable energy sources is needed to meet the same. Besides, traditional energy sources cause a hazard to human health by generating greenhouse gases. Therefore, the world needs a power source that is less pollutant, highly efficient, and high capacity for energy supply to meet the global demand for an energy crisis (Eigenbrodt et al. 2011; Ji et al. 2015). The internal combustion engine (ICE) has been considered the most popular energy conversion device for various applications, from transportation to electric power supply, for an extended period. The hydrocarbons are used as fuel for the same device. But, several drawbacks of the ICE have been realized by a large number of scientists, including emission of most common greenhouse gas (CO<sub>2</sub>), very low efficiency of energy conversion about 15–25%, generation of several unwanted by-products, creation of unwanted noise, and generation of power from non-renewable fuels (Yang et al. 2015; Pan et al. 2019).

A few sustainable technologies, such as solar power, wind power, tidal energy, and hydropower can supply clean energy by utilizing renewable energy. Fuel cell technology is one of the most promising technologies that can use renewable energy to produce power with high efficiency. The fuel cell converts chemical energy into electrical energy without directly burning the fuel, eliminating greenhouse gas emissions such as CO<sub>2</sub> and CO in the environment (Hassen et al. 2016a; Zhao et al. 2017; Zhang et al. 2020). Fuel cell technology is one of the most promising technology among them that can utilize renewable energy sources to produce electricity with high efficiency. The fuel cell converts the chemical energy of fuel into electrical energy without the direct combustion of fuel which eliminates or decreases the emission of greenhouse gases like CO<sub>2</sub> and CO in the environment. Fuel cell technology is one of the most promising technologies for increasing renewable energy production because fuel cells have higher efficiency than conventional combustion devices (Hao et al. 2017; Lu et al. 2018; Hanif et al. 2021). The efficiency can be increased further by using the produced heat. Fuel cells are distinguished from other traditional energy conversion devices by their high energy conversion efficiency and low pollutant emission (Sundmacher 2010; Qiao et al. 2020). Furthermore, compared to traditional energy generation methods, fuel cell operation is vibration-free, resulting in less noise pollution. Recently,

several researchers have shown interest in developing various types of fuel cells because of their high efficiency, negligible noise, simple design, sustainability, and easy scalability. Various types of fuel cells are available depending on electrolyte, fuel, and operating temperature. There are various fuel cells available in the market such as hydrogen fuel cells (Chen et al. 2017), direct methanol fuel cells (Huang et al. 2022), and microbial fuel cells (Tran et al. 2022). Despite having a lot of constraints that must be solved, all existing fuel cells offer a significant promise to create clean, sustainable energy with high energy conversion efficiency (Kang et al. 2017; Son et al. 2021; Zahid et al. 2022). In addition, fuel cells are categorized as polymer electrolyte fuel cells, solid oxide fuel cells, phosphoric acid fuel cells, alkaline fuel cells, and molten carbonate fuel cells based on the type of electrolytes employed. Among various fuel cells, solid oxide fuel cells (SOFCs) are considered the most desirable fuel cell for generating electricity from hydrogen and hydrocarbons (Muñoz-García et al. 2014; Xu et al. 2020). Figure 1 depicts the number of articles published each year on SOFCs from 2011 to 2020. In the twenty-first century, fuel cells are the most promising, silent, and eco-friendly source of electrical energy (Lucia 2014). The major evolutionary changes that occur during the development of fuels can be summarized according to Table 1. This green technology came into existence in 1839 when the fuel cell was invented by Sir William R. Grove. In 1889, Ludwig Mond and Carl Langer developed a new form of gas batteries where they used hydrogen to produce electricity and introduced the name “fuel cell” for the first time. In 1959, Francis Thomas Bacon (Andújar and Segura 2009) successfully constructed a stack of 40 fuel cells that could develop 5 kW of electrical power. After 100 years of invention, Pratt and Whitney (Williams 1994) modified the Bacon’s cell to install in the Apollo space vehicle that enabled astronauts to land on the moon in 1969 as an efficient technology for power generation and to provide drinking to the crew members. It continued a long history in itself to flourish for market application in the present scenario. Today, scientist and technologist all over the world are working to commercialize fuel cells to meet the local and global energy needs.

Among the different kinds of available fuel cells, solid oxide fuel cells (SOFCs) have achieved great attention in various applications such as transportation and stationary electrical power supply because of their high fuel flexibility, efficiency, durability, and simple design (Liu et al. 2014; Hua et al. 2016; Chen et al. 2019). Solid oxide fuel cell (SOFC) systems are the best choice for stationary high-power energy generation among the different types of fuel cells (Chao et al. 2011; Xia et al. 2016). As solid electrolytes, SOFCs use ceramic materials that can conduct oxygen ions or protons. In addition, SOFCs use various ceramic and ceramic–metal composite materials

**Fig. 1** Number of articles published each year on SOFCs from 2011 to 2020. Google Scholar was used to search using the term “solid oxide fuel cell”

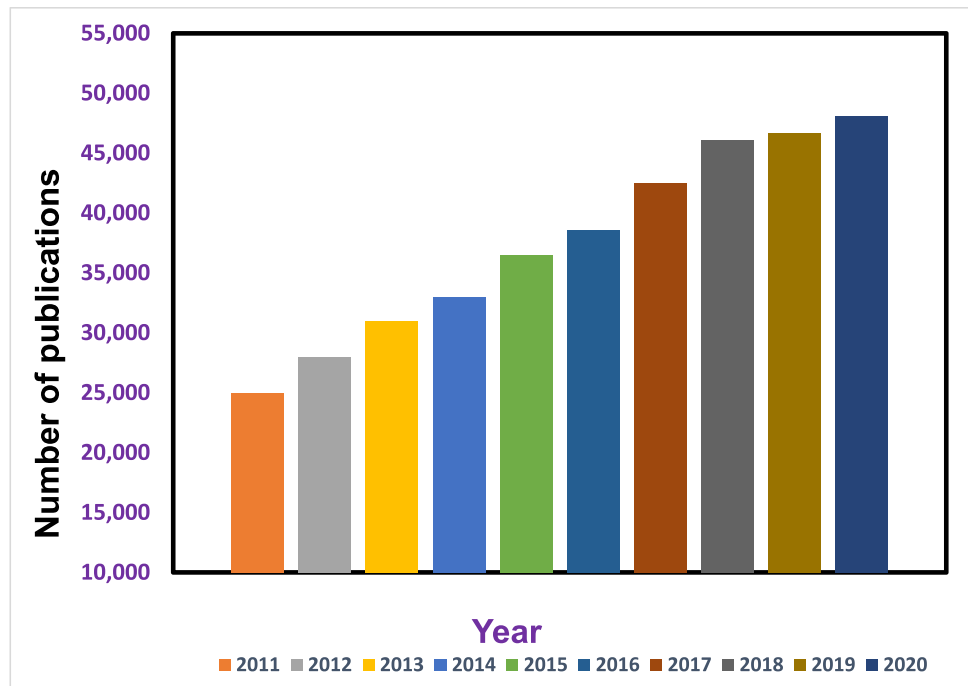


**Table 1** Key developments the field of in fuel cell technology

Years	Invention	Reference
1839	The first fuel cell was created by William Grove (1811–1896). He called it a “gas voltaic battery.”	(Andújar and Segura 2009)
1889	Charl and Mond built on Grove’s created a fuel cell that can generate 2 A current	(Grimes 2000)
1893	The theoretical performance of fuel cells was discussed Ostwald	(Abdalla et al. 2018)
1939	Bacan created alkaline fuel cells (AFCs) with a high-power density (1.11 A/cm <sup>2</sup> at 0.6 V)	(Perry and Fuller 2002)
1959	The proton exchange membrane fuel cell was created by General electric	(Jamil et al. 2022)
1961	Nafion membrane were created by DuPont	(Perry and Fuller 2002)
1969	Fuel cell technology was utilized in space by NASA	(Steele 2001)
1990	A direct methanol fuel cell has been created for the first time	(Dadashzadeh et al. 2016)
2007	Honda announced to produce fuel cell car	(Morikawa et al. 2009)
2009	In Japan, portable fuel cell battery chargers were widely available	(Wilberforce et al. 2016)
2014	Toyota introduced the first commercial fuel cell vehicle	(Yoshida and Kojima 2015)

such as cathode and anode. SOFCs function at high temperatures, often between 800 and 1000 °C (Wei et al. 2018; Yang et al. 2020). In contrast to low-temperature fuel cells, which have poor impurity tolerance and can only use high-purity hydrogen, high-temperature fuel cells (such as SOFCs) can use a variety of fuels, including H<sub>2</sub>, CO, CH<sub>4</sub>, and C<sub>2</sub>H<sub>6</sub>. On the other hand, the high working temperatures of SOFCs place restrictions on the materials (functional and structural components) utilized in the cells. For example, electrolytes, electrodes, and interconnects should all have identical linear coefficients of thermal expansion in order for the SOFC to heat up from room temperature to working temperatures without cracking due to thermal expansion mismatch. Furthermore, high

operating temperatures lengthen fuel cell-based systems’ start-up and cool-down times, reducing their commercial viability. In addition, chemical reactions between the electrolyte and the electrode materials are more likely to occur at high temperatures. The properties of the fuel cell deteriorate as a result of these reactions, and the cell lifetime decreases. Due to the limitations of high-temperature SOFCs, several research groups are focusing on the development of intermediate-temperature SOFCs which can operate at intermediate temperatures (600–800 °C). The intermediate-temperature SOFCs’ low working temperatures remove limits on the thermal expansion properties of the materials utilized, allowing for faster start-up and cool-down times. However, the low working temperatures

have several disadvantages. Reaction rates at electrodes in the intermediate-temperature SOFCs are lower which reduces the fuel cell efficiency. In addition, ionic conductivity in solid oxide electrolyte is significantly reduced at lower temperatures. As seen by the growing number of publications in this field, there has been much interest in developing materials for intermediate-temperature-SOFCs in recent years which could bring appropriate solution of the current problem of intermediate-temperature SOFCs (He et al. 2017; Wei et al. 2017; Yang et al. 2020). An ion-conducting electrolyte, an anode, and a cathode are the basic components of a fuel cell, as shown schematically in Fig. 2a. Figure 2b–c shows a planar and a tubular of SOFC. The planar SOFC design is a commonly utilized in single cell fabrication because it allows to achieve high fuel cell performance while keeping the manufacturing process cost low. In general, companies have used the planar SOFC design since it is less expensive and takes less time to produce each component than the tubular SOFC design. Furthermore, this architecture is appropriate for developing a tiny SOFC stack for portable applications. The working principles of oxygen ion-conducting SOFCs (O–SOFC) and proton-conducting SOFCs (P–SOFC) are compared in Fig. 2d–e. P–SOFCs have potential to achieve high performance at low temperatures because proton conduction in solid oxides has a lower activation energy than oxygen-ion conduction. The development of a suitable electrolyte is essential for the commercialization

of SOFCs. Doped  $\text{Bi}_2\text{O}_3$ ,  $\text{CeO}_2$ ,  $\text{ZrO}_2$ , and  $\text{LaGaO}_3$ -based materials have been extensively investigated as solid oxide electrolytes for fuel cell applications.

According to previous research reports, all forms of solid oxide electrolyte materials have advantages and disadvantages that may be related to the materials' fundamental characteristics. The role of various components, operating principles, and potential applications of SOFCs has been discussed in the first section of this review. Subsequently, this article highlights various recent advancements in solid oxide electrolytes which has been used in fuel cells, particularly zirconia- and ceria-based electrolytes, as major advancements toward sustainable and clean energy production because zirconia- and ceria-based electrolytes are regarded as the most promising electrolyte material for SOFCs due to their various properties, including excellent ionic conductivity, superior chemical, mechanical, and thermal stability over a wide temperature range, and good compatibility with the other cell components. Various successes, prospects, and challenges of zirconia- and ceria-based electrolytes for the practical implementation in SOFCs have been reviewed as important steps toward achieving sustainable and clean energy production. Its relevance in the current global energy crisis and environmental pollution is thought to be quite effective.

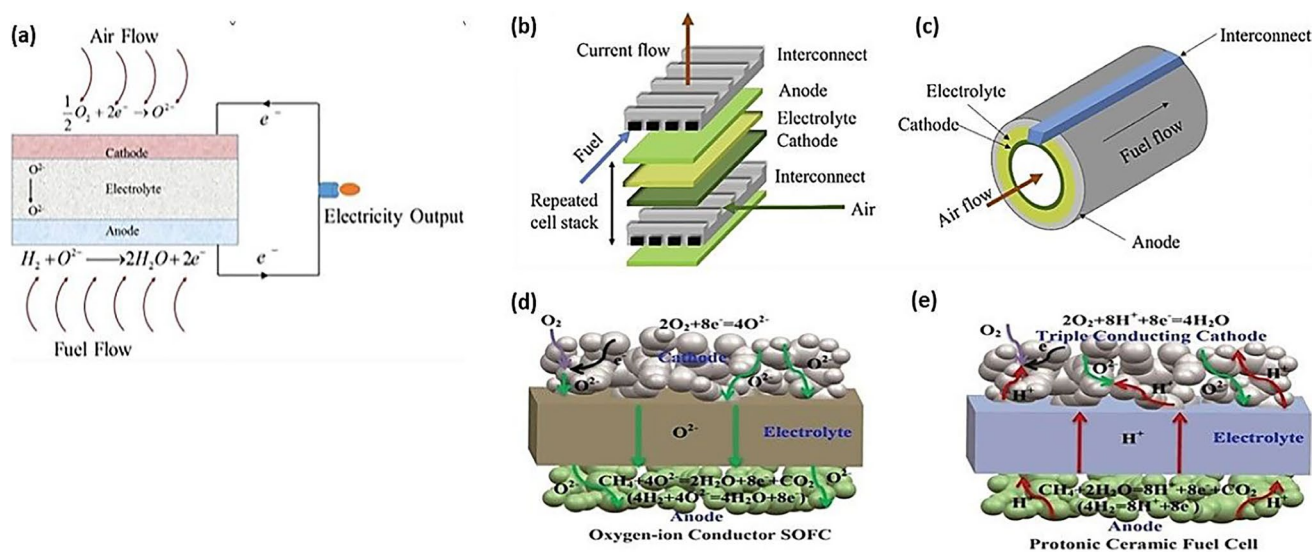


**Fig. 2** a Schematic of a SOFC, b Schematic of a planar SOFC unit, c a tubular SOFC unit (Ng et al. 2019). Reproduced with permission from the ref. (Ng et al. 2019), Copyright 2019 Elsevier, working

principle of d oxygen ion-conducting SOFC unit, e proton-conducting SOFCs (Duan et al. 2015). Reproduced from the ref. (Duan et al. 2015)

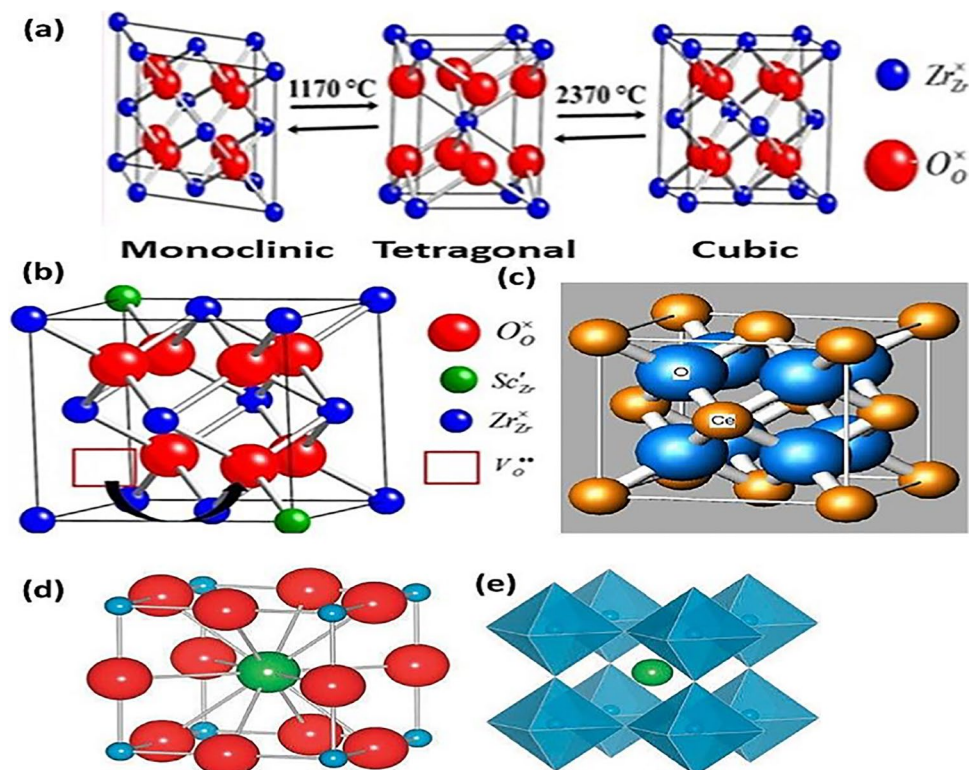


## Solid oxide electrolyte used in fuel cells

The main components of a single SOFC unit are cathode, anode, and electrolyte. The solid oxide electrolyte, which conducts oxygen ions, is the most significant component of a SOFC unit. In general, the required features of each SOFC component are comparable for every application, ranging from large-scale to small-scale. Interconnect is used in the stack of SOFCs to create an electrical connection between single cells. The number of cells in the stack of SOFCs depends on the required output for particular applications (Chao et al. 2011; Ghezal-Ayagh et al. 2013; Chen et al. 2017). For large-scale applications of SOFCs, the size and the number of single cells should be large enough to generate the required power. In contrast, for portable applications of solid oxide fuel cells (SOFCs), the cell size should be small enough to carry from one location to another (Sandhu et al. 2016; Abdalla et al. 2018; Afroze et al. 2019; Khan et al. 2020). The requirement properties and the function of the component are illustrated in the following section. The electrolyte is sandwiched between the porous cathode and the porous anode in a conventional SOFC, and it serves as following key functions: (i) it separates the anode and cathode gases and (ii) it transfers ions between the anode and the cathode. Electrolytes should have excellent ionic conduction, high compactness, and chemical and thermal stability to attain

high SOFC performance. SOFCs can be classed based on type of ion conduction through electrolyte as (i) oxygen ion-conducting SOFCs (O-SOFC), where oxygen ions are transported through the electrolyte, (ii) proton-conducting SOFCs (P-SOFC), where protons are transported through the electrolyte, and (iii) dual ion conducting SOFCs (D-SOFC), where both protons and oxygen ions are transported through the electrolyte. The solid oxide electrolyte, which conducts oxygen ions, is the most significant component of a SOFC unit. It is the heart of SOFC. The use of zirconia-based electrolytes as an electrolyte material in SOFCs has been extensively investigated. Pure zirconia exhibits three crystallographic polymorphs (as shown in Fig. 3a). At room temperature, monoclinic (*m*) is the stable form of zirconia. During heating *m*-ZrO<sub>2</sub> to *t*-ZrO<sub>2</sub> and *t*-ZrO<sub>2</sub> to *c*-ZrO<sub>2</sub>, phase transformations occur at 1170 °C and 2370 °C, respectively. The cubic form is stable up to its melting point (2680 °C). All these phase transformations are reversible on cooling, although the temperature at which the tetragonal to monoclinic phase transformation occurs during cooling is somewhat lower (950–1000 °C) (Badwal 1992; Fini et al. 2018). For an oxygen ion conductor, conduction occurs via the oxygen vacancy hopping mechanism. In the hopping mechanism, oxide ion jumps from its original tetrahedral site to an adjacent oxygen vacant site, and a counter migration of ions and vacancies takes place, as shown in Fig. 3b (Mahato et al. 2015). Oxygen ion diffusion is achieved by creating oxygen vacancy

**Fig. 3** **a** Polymorphism of zirconia, **b** schematic showing oxygen vacancy hopping mechanism in fluorite structured Sc<sub>2</sub>O<sub>3</sub>-doped ZrO<sub>2</sub>, **c** cubic fluorite crystal structure of ceria (Anwar et al. 2016). Adopted from the ref. (Anwar et al. 2016) **d–e** cubic perovskite structure of LaGaO<sub>3</sub> (Malavasi et al. 2010). Reproduced from the ref. (Malavasi et al. 2010)



defects inside the lattice. Examples of such crystal structures with predominant oxygen vacancy are doped  $\text{Bi}_2\text{O}_3$ ,  $\text{CeO}_2$  (Fig. 3c), and  $\text{ZrO}_2$ -based oxides with fluorite structure,  $\text{LaGaO}_3$ -based perovskites (Fig. 3d–e),  $\text{Bi}_4\text{V}_2\text{O}_{11}$ , and  $\text{La}_2\text{Mo}_2\text{O}_9$ -based derivatives (Ishihara et al. 2006; Guan et al. 2015). The main requirements for the material to be used as the electrolyte in SOFC are high oxide ion conductivity, chemical stability, and mechanical stability.

Most of the highly ionic conductive oxide materials possess cubic fluorite structures. The interstitial octahedral site of cubic fluorite remains unoccupied, which results in a relatively open crystal structure. These unoccupied interstitial sites give an easy pathway for oxygen ion conduction and make the oxide favorable as an anionic conductor (Kharton et al. 2004). Ceria-based electrolytes exhibit higher ionic conductivity than the doped zirconia-based electrolyte, but the reduction of  $\text{Ce}^{4+}$  cations, present in ceria, to  $\text{Ce}^{3+}$  under a typical SOFC anode condition leads to the lowering of open circuit potential and performance of cells (Yasuda et al. 2012). The next higher conducting oxide is doped zirconia, which possesses good mechanical stability in both oxidizing and reducing atmosphere. Scandia-stabilized zirconia (ScSZ) has shown the highest ionic conductivity (Fig. 4) among doped  $\text{ZrO}_2$  systems because of the similar ionic radius of  $\text{Sc}^{3+}$  and  $\text{Zr}^{4+}$ . It has been reported that at 850 °C, the ionic conductivity of 11 ScSZ is 108 mS/cm, which is 1.5 times higher than the conductivity of 8 mol. % yttria-stabilized zirconia (8YSZ) (78 mS/cm) (Badwal and Ciacchi 2000). However, the conductivity of 11ScSZ drops suddenly around 600 °C due to the transformation from a highly conductive, vacancy-disordered, and cubic fluorite phase

to a low conductive, vacancy-ordered, and rhombohedral  $\beta$ -phase (Politova and Irvine 2004). In addition, the presence of multiple poor conducting and metastable phases in lower Sc2O3 (5–9 mol. %) containing compositions adversely affect the overall conductivity of ScSZ electrolytes (Fujimori et al. 1998). In the composition range of 5–7 mol. % Sc2O3-ZrO2, tetragonal phase is present with lower symmetry monoclinic phase, which is a poor conducting phase (Fujimori et al. 1998). In 7–9 mol. % Sc2O3, phase composition consists of a metastable  $t'$  and  $t''$ -phase along with a stable tetragonal phase (Badwal et al. 2000). The ionic conductivity of the metastable  $t'$ -phases decays with annealing as it decomposes to a Sc-rich cubic matrix and fine precipitates of Sc-deficient lower conducting tetragonal phase at the fuel cell operating temperature (800–1000 °C). The high conducting cubic phase is stable in a very narrow range of Sc2O3 doping concentration (9–10 mol. % Sc2O3) (Ruh et al. 1977). Since cubic is the highest conducting phase of doped zirconia, a second dopant, i.e., co-dopant ( $\text{CeO}_2$ ,  $\text{Y}_2\text{O}_3$ ,  $\text{Yb}_2\text{O}_3$ ,  $\text{Al}_2\text{O}_3$ ,  $\text{Ga}_2\text{O}_3$ , etc.), is typically added to improve the stability of cubic phase over other lower conducting and metastable phases (Zhuiykov 2000; Arachi et al. 2001; Omar et al. 2012). It has been reported that 1 mol. %  $\text{CeO}_2$  co-doped with 10 mol. % Sc2O3-ZrO2 system shows the highest ionic conductivity (16.7 mS/cm) at 600 °C (Omar et al. 2012). This phase composition shows no phase transition or oxygen vacancy ordering phenomena in aging at high temperatures (Lee et al. 2005). The effect of 1 mol. %  $\text{CeO}_2$  addition on phase stability and ionic conductivity in the Sc2O3-ZrO2 system at low Sc2O3 concentration (5–9 mol %) is still unexplored. In this study, 1 mol. %  $\text{CeO}_2$  has been co-doped in ScSZ system to stabilize the high symmetry phases at lower scandia content (5–11 mol. %) and thereby increase ionic conductivity. Lowering the Sc2O3 content in ScSZ system improves the mechanical property (Fleischhauer et al. 2015) and lowers the cost of fabrication since the cost of Sc2O3 is 10 times more than the cost of  $\text{CeO}_2$  and  $\text{ZrO}_2$  (Kumar et al. 2016). Lowering the scandia content also reduces the effect of local defect structures on lowering the ionic conductivity which is significantly high at higher doping concentration (greater than 10 mol. % Sc2O3) (Omar et al. 2008).

In the case of proton-conducting electrolytes, proton diffusion requires less activation energy than the transportation of oxygen ions. As a result, it is easier to achieve higher proton conductivity than oxygen ion conductivity at lower and intermediate temperatures. The conductivity of oxygen ions of ceramic electrolytes often decreases quickly as the operating temperature drops due to the high activation energy ( $E_a$ ) of oxygen ion conduction. As a result, proton-conducting solid oxide materials are more appropriate as intermediate and low-temperature electrolytes than oxygen ion-conducting solid oxide electrolytes. The vehicle mechanism and the

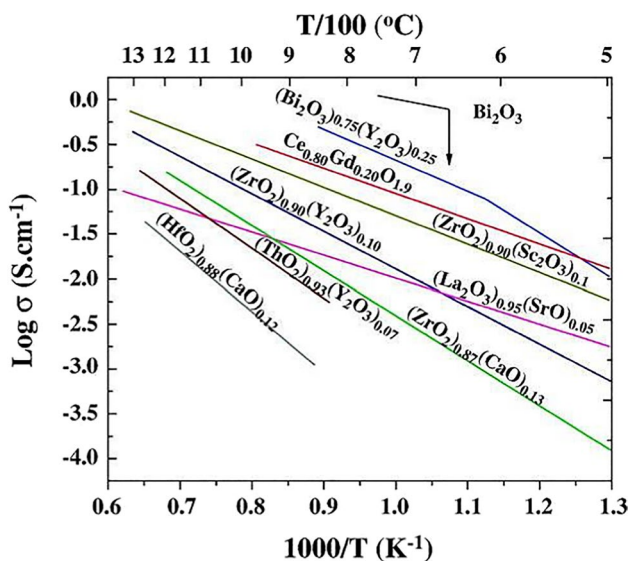


**Fig. 4** Ionic conductivity in fluorite structure oxides at different temperatures (Omar et al. 2006). Reproduced with permission from the ref. (Omar et al. 2006). Copyright 2006 Elsevier

Grotthuss method are the two basic proton transport mechanisms for proton-conducting electrolytes (Cao et al. 2021). Until now, the most common proton-conducting electrolytes are BaCeO<sub>3</sub> and BaZrO<sub>3</sub>-based materials. The oxygen vacancies are linked to proton conduction in perovskite-type crystal structures. In addition, mixed oxygen ion and proton conduction may arise inside these perovskite oxides, leading to the development of dual ion-conducting SOFCs. According to previous research, all three types of accessible oxygen ion-conducting electrolyte materials have flaws, which could be related to the materials' inherent properties (Irshad et al. 2016; Rashid et al. 2019; Vostakola and Horri 2021). Proton-conducting electrolytes have low activation energy and can be employed at low operating temperatures. As a result, developing a suitable electrolyte for SOFC is critical for the commercialization of fuel cell technology. The following section shows various advancements in solid oxide electrolytes used in fuel cells, particularly zirconia- and ceria-based electrolytes.

## Zirconia-based electrolyte used in fuel cells

Zirconia-based materials are the most commonly used electrolytes because of their outstanding mechanical and chemical durability and reasonable oxygen ion conductivity. Among the many types of electrolyte materials, yttria-stabilized zirconia (YSZ)-based electrolyte materials are the most widely researched for SOFC applications. YSZ-based electrolytes are most widely explored for SOFC applications among the various type of electrolyte materials because of their acceptable ionic conductivity (Vostakola and Horri 2021). YSZ becomes an oxygen ion (O<sup>2-</sup>) conductor above 800 °C; zirconia-based SOFCs perform in a temperature range of 800 to 1100 °C. The contribution of the electrolyte to the ohmic loss in the SOFC is maintained to a minimum with a thin electrolyte (25–50 μm). Many factors influence the ionic conductivity of zirconia-based electrolytes, including dopant concentration, defect dissociation, sample preparation, oxygen partial pressure, and temperature. In order to promote high oxide ion conductivity, all the oxygen ions should have equal or similar energy. Thus, high symmetry structures are preferred for oxygen ion conduction. As a result, the cubic phase of zirconia should be stabilized to use as a solid oxide electrolyte. In the cubic fluorite structure, cations form the face-centered cubic sub lattice, while the oxygen ions occupy all the tetrahedral sites. The octahedral sites remain unoccupied which provide an easy pathway for oxygen-ion conduction. However, the size of Zr<sup>4+</sup> cation is too small to retain the cubic fluorite structure (Chen et al. 2016b; Vostakola and Horri 2021). Thus, doping with larger cation stabilize the cubic structure in ZrO<sub>2</sub>. Furthermore, the incorporation of anion vacancies in the lattice by doping

with acceptor dopant can reduce the repulsion between anions and stabilize the fluorite phase. These metal cations substitute the Zr<sup>4+</sup> cation to create oxygen vacancies as a charge compensating defects (Shimada et al. 2017; He et al. 2018; Hou et al. 2019; Wei et al. 2019). Scandia-stabilized zirconia (ScSZ) is the most promising candidate for the electrolyte application in SOFC as it possesses highest ionic conductivity among doped ZrO<sub>2</sub> system. ScSZ materials have a high ionic transference over a wide temperature range and good thermomechanical properties, allowing them to work at lower temperatures (Aguadero et al. 2012; Mahato et al. 2015; Ito et al. 2019). Doping of Sc<sub>2</sub>O<sub>3</sub> in ZrO<sub>2</sub> creates oxygen vacancy. This oxygen vacancy is responsible for the ionic conduction in ScSZ system. Thus, with the increase in scandia dopant concentration, the concentration of oxygen vacancy also increases resulting in an increase of ionic conductivity. However, at a certain dopant concentration, ionic conductivity goes through a maximum after which it decreases. The oxygen vacancies tend to interact with dopant cations at high dopant concentrations (> 10 mol%) (Bhattacharyya and Omar 2018; Sudarsan and Krishnamoorthy 2018). These interactions result in a local defect structures or complex defect associates, which reduces the effective number of mobile oxygen vacancies and consequently decreases the conductivity.

Apart from high initial ionic conductivity, minimal conductivity degradation at operating temperature is equally important for the electrolyte material. The conductivity deterioration of electrolytes should not exceed 0.1% per 1000 h (Accardo et al. 2017; Kumar et al. 2020). The cubic phase shows the highest ionic conductivity and lower conductivity degradation in aging in Sc<sub>2</sub>O<sub>3</sub>-ZrO<sub>2</sub> system. A second dopant (Y<sup>3+</sup>, Yb<sup>3+</sup>, Al<sup>3+</sup>, Ga<sup>3+</sup>, Gd<sup>3+</sup>, etc.) has been added within the Sc<sub>2</sub>O<sub>3</sub>-ZrO<sub>2</sub> system to improve the stability of cubic phase over rhombohedral β-phase at room temperature and to inhibit the transformation from cubic to vacancy ordered β-phase during the aging of electrolyte (Kumar et al. 2017; Nikonov et al. 2017). Politova and Irvine (2004) have shown that only 1 mol. % addition of Y<sub>2</sub>O<sub>3</sub> in (Y<sub>2</sub>O<sub>3</sub>)<sub>x</sub>(Sc<sub>2</sub>O<sub>3</sub>)(11 - x)(ZrO<sub>2</sub>)<sub>89</sub> system successfully stabilized the cubic phase over rhombohedral β-phase, which results in a linear Arrhenius plot of conductivity without any step. A similar type of cubic phase stabilization effect and linear Arrhenius plot was also observed by Arachi et al. (2001) on the addition of CeO<sub>2</sub> and Ga<sub>2</sub>O<sub>3</sub> as a co-dopant in the Sc<sub>2</sub>O<sub>3</sub>-ZrO<sub>2</sub> system. The effect of CeO<sub>2</sub> addition on phase stability and conductivity behavior in the Sc<sub>2</sub>O<sub>3</sub>-ZrO<sub>2</sub> system has been well studied by several researchers. Lee et al. (2005) have reported that the addition of 1 mol. % CeO<sub>2</sub> in 10ScSZ composition successfully stabilizes the cubic phase. It is also reported that this composition possesses much higher ionic conductivity in the temperature range of 300–1100 °C and better long-term stability than



other Sc<sub>2</sub>O<sub>3</sub>-ZrO<sub>2</sub>-based electrolytes. Wang et al. (Wang et al. 2005) have shown that the addition of CeO<sub>2</sub> beyond 1 mol. % in 10ScSZ leads to a decrease in conductivity due to an increase in lattice strain. Omar et al. (2012) have also reported that CeO<sub>2</sub> co-doped with Sc<sub>2</sub>O<sub>3</sub>-ZrO<sub>2</sub> shows far better conductivity among the various co-dopant used for phase stabilization in Sc<sub>2</sub>O<sub>3</sub>-ZrO<sub>2</sub> system. Solid oxide electrolytes as oxygen ion conductors are of tremendous interest in various research areas, including solid oxide fuel cells (Smeacetto et al. 2010; Hanif et al. 2021), ionic membranes (Kerman and Ramanathan 2014), and gas sensors (Park et al. 2003). Stabilized zirconia-based electrolytes are perhaps the most well-known oxygen ion conductor. At high temperatures, stabilized zirconia-based electrolytes possess good ionic conductivity and extraordinary mechanical and chemical stability. For SOFC applications, numerous materials have been investigated as electrolytes for fuel cell applications; the most frequent materials utilized for the oxide-conducting electrolyte are YSZ and gadolinium-doped ceria (GDC). YSZ becomes an oxygen ion (O<sup>2-</sup>) conductor above 800 °C; zirconia-based SOFCs perform in a temperature range of 800 to 1100 °C. At 1000 °C, YSZ has an ionic conductivity of approximately 0.1 to 0.2 S cm<sup>-1</sup> (Xu et al. 2020; Hanif et al. 2021; Huang et al. 2021). The contribution of the electrolyte to the ohmic loss in the SOFC is maintained to a minimum with a thin electrolyte (25–50 μm). Many factors influence the ionic conductivity of zirconia-based electrolytes, including dopant concentration, defect dissociation, sample preparation, oxygen partial pressure, and temperature (Shimada et al. 2019; Ren et al. 2020b; Xu et al. 2020). In ZrO<sub>2</sub>-based systems, ionic conductivity initially rises with rising concentrations of acceptor dopant cations up to a certain level. It is widely accepted that the oxygen ion conductivity of YSZ is highest when the Y<sub>2</sub>O<sub>3</sub> content is ~8 mol.%. As the dopant concentration rises further (above 8 mol.% of the Y<sub>2</sub>O<sub>3</sub>), the flow of mobile oxygen vacancies is slowed, resulting in a decrease in oxygen ion conductivity (Hao et al. 2017; Singh and Chavan 2019; Li et al. 2021). The oxygen ion conductivity of typical 8 mol % Y<sub>2</sub>O<sub>3</sub>-stabilized ZrO<sub>2</sub> (YSZ) is suitable for fuel cell applications at 1000 °C; however, the oxygen ion conductivity of YSZ is dramatically lowered with lower temperatures (Yamamoto et al. 1995; Smeacetto et al. 2010). On the other words, the ionic conductivity of these electrolytes at intermediate temperatures is insufficient for most technical applications, necessitating the search for ways to increase it. As a result, novel ways either to increase the conductivity of existing materials or develop new electrolyte materials are required for their realistic application in intermediate temperatures.

Nanostructuring or changing the shape and grain size of solid electrolytes is an obvious technique for enhancing ionic conductivity. The improvement in ionic conductivity of the YSZ electrolyte of up to two orders of magnitude has been

documented using this method. In certain situations, there has been no improvement in ionic conductivity. As a result, the conductivity of nanoscale YSZ has a wide range of values. The challenge of managing both the microstructure and the chemical composition of grain boundaries in polycrystalline ceramics is one of the main reasons for the disparities in results. The ionic conductivity of zirconia solid electrolytes is determined by both the type and concentration of doping oxide. The conductivity reaches its peak at a given dopant concentration (as shown in Fig. 5). The maximum ionic conductivity is noticed in YSZ at roughly 8 mol% yttria, which is considered the low-concentration boundary for the phase stability of cubic zirconia. In the case of scandia-doped zirconia (ScSZ), maximum ionic conductivity is observed at a doping concentration of 10–11 mol%. It is observed that the position of the maximum is related to the difference in ionic radii between the dopant cation and Zr<sup>4+</sup>. The lower the dopant concentration is needed to attain maximal conductivity when the radii difference is greater. YSZ is the most extensively utilized electrolyte for high-temperature SOFCs among zirconia-based materials because it has a sufficiently good ionic conductivity at high temperatures, 0.12 S/cm at 1000 °C (Wang et al. 2019), and low-cost in comparison to other zirconia-doped electrolytes. At working temperatures of 500–600 °C, the ionic conductivity of YSZ is insufficient; it is only around 0.001 S/cm. Because of the low activation energy for oxygen vacancy diffusion, scandia-stabilized zirconia electrolyte (ScSZ) has better ionic conductivity than YSZ (Ng et al. 2016; Azim Jais et al. 2017).

However, ScSZ has several drawbacks, such as being more expensive than YSZ and deterioration under operating conditions. ScSZ electrolyte deterioration is more noticeable when scandia doping levels are less than 8 mol% (Haering et al. 2005; Spirin et al. 2012). Although ScSZ electrolytes

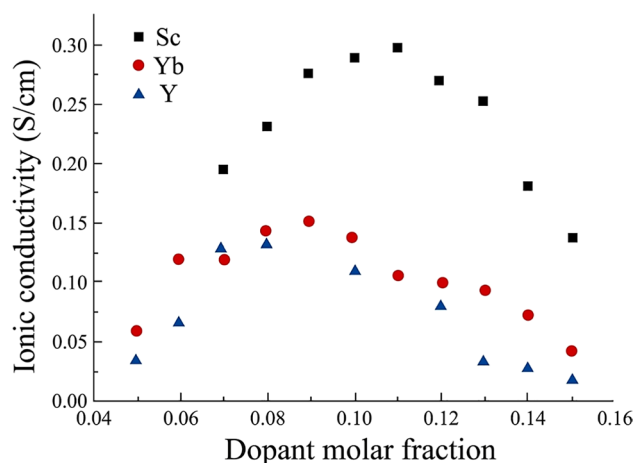


**Fig. 5** Variation of the ionic conductivity of zirconia-based electrolytes depending upon doping concentration at 1000 °C (Zhigachev et al. 2021). Reproduced from the ref. (Zhigachev et al. 2021)



with 10–12 mol% show the highest measured conductivity, it has drawbacks as well. When these electrolytes are cooled to 500–700 °C, the cubic zirconia phase converts into a rhombohedral phase with ordered oxygen vacancies, which has a conductivity at least an order of extent lower than the cubic phase (Arachi et al. 1999). As a result, the use of ScSZ electrolytes in IT-SOFCs is restricted until a solution for suppressing the cubic to rhombohedral phase transformation while chemical stability and maintaining ionic conductivity are discovered. Voltage vs. current density plot are very important to understand the performance of a fuel cell. There are three types of voltage losses in a fuel cell polarization curve are as follows: mass transport losses, ohmic losses, and activation polarization losses. The reaction kinetics occurring at the electrodes is the primary source of activation polarization losses. Resistances in the materials employed in the cell are the primary cause of ohmic losses (Qiao et al. 2018; Xia et al. 2018; Masciandaro et al. 2019). The incapability to provide enough reactants to the catalyst layers of the electrodes to meet demand is the primary source of mass transport losses. Developments of

the right materials for fuel cells can reduce all three types of losses. For example, enhancements in oxygen ion conductivity might minimize ohmic losses, whereas improvements in catalytic activity could reduce activation polarization losses (Khan et al. 2018; Nielsen et al. 2018; Riegraf et al. 2021). The electrolyte in SOFCs is critical in determining the operating temperature and overall conversion efficiency. Various ion conductors have been used as electrolytes in SOFCs, including gadolinium-doped ceria (GDC) and yttrium stabilized zirconia (YSZ). Despite the fact that SOFCs are the most efficient method of converting chemical energy into usable electrical energy, their commercialization has been restricted by their high operating temperatures (800–1000 °C) (Chen et al. 2016a; Shin et al. 2021). Despite the excellent ionic conductivity of doped ceria, ceria-based electrolytes have several drawbacks when working at intermediate temperatures. However, SOFCs' electrochemical performance degrades rapidly in the lower temperatures. As a result, developing high-performance IT-SOFCs is essential to expanding their commercial application potential (Fu et al. 2021; Istomin et al. 2021). A new form of bismuth

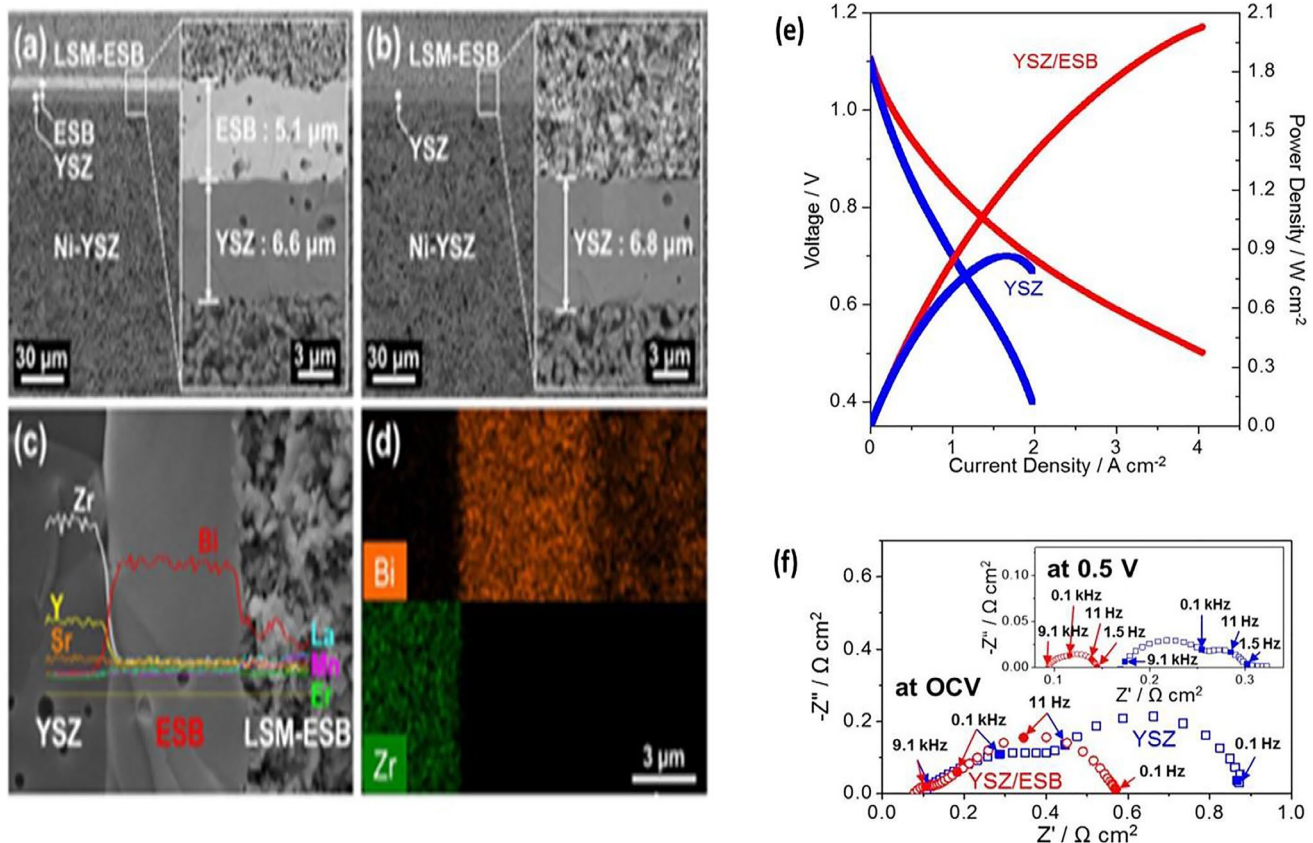


**Fig. 6** SEM images of **a** ESB/YSZ bilayer SOFC unit, **b** YSZ single layer SOFC unit. EDS analysis with **c** line-scan, and **d** areal elemental mapping of the YSZ/ESB/LSM-ESB, **e** fuel cell performance test using YSZ and YSZ/ESB electrolytes at 700 °C, where YSZ and ESB

represent  $Y_{0.16}Zr_{0.8}O_{1.92}$ , and  $Bi_{1.6}Er_{0.4}O_3$ , respectively (Joh et al. 2017), **f** Nyquist plots at 0.5 V OCV. Reproduced from the ref. (Joh et al. 2017). Copyright 2017 ACS

oxide/zirconia bilayer (ESB/YSZ) electrolyte for SOFCs was developed by Joh and colleagues (Joh et al. 2017). Figure 6a and b show the cross-sectional SEM images of SOFCs made of ESB/YSZ bilayer and YSZ single layer electrolytes, respectively. These SEM micrographs have revealed that both cells have the similar structure, with the exception of the extra ESB layer. The findings have proved that using a simple screen-printing technique, the ESB layer can be uniformly coated on the YSZ surface without generating any pores. Energy dispersive X-ray spectroscopy (EDS) was used to analyze the composition (Fig. 6c) and the areal mapping in order to evaluate any potential interdiffusion of constituent elements between layers (Fig. 6d). The resulting spectra show that there is no interdiffusion of any components between layers. The electrochemical impedance spectra of the two cells are shown in Fig. 6f. The high frequency intercepts at the real axis were used to measure ohmic losses using Nyquist plots. Due to the substantially enhanced oxygen incorporation process at the cathode/electrolyte interface, the new bilayer (ESB/YSZ)-based SOFC delivers an exceptionally high-power density of 2.1 W/cm<sup>2</sup> at 700 °C, which is 2.4 times greater than the YSZ single electrolyte SOFC, as shown in Fig. 6e. The output voltage remained constant for 150 h, demonstrating that the ESB/YSZ bilayer SOFC is very stable in the intermediate temperature range. This study revealed that the bilayer electrolyte is a potential alternative electrolyte for achieving greater power density SOFCs at lower temperatures.

Yttria-stabilized zirconia (YSZ)-based materials are commonly employed as electrolytes in SOFCs due to their outstanding chemical stability and mechanical strength in reducing and oxidizing atmospheres and good oxide ion conductivity at operating temperatures (Hao et al. 2017) (Abdalla et al. 2018). Compared to other solid oxide electrolyte materials such as doped ceria and bismuth oxides, YSZ has low oxide ion conductivity at low temperatures. In order to resolve this issue, YSZ electrolytes are often manufactured as thin films to reduce the ohmic loss caused by the poor ionic conductivity of electrolytes. In a research study, Cho and his colleagues (2019) developed YSZ-based thin-film electrolytes with variable Y<sub>2</sub>O<sub>3</sub> doping concentrations for SOFC applications. TEM analysis has been performed in order to observe into the specific microstructures of thin-film SOFCs. According to the well-known inherent characteristics of ALD films, it is clearly visible that all of the deposited YSZ thin-film electrolytes exhibit a partially polycrystalline structure (Fig. 7b–f) and similar porosity regardless of Y<sub>2</sub>O<sub>3</sub> concentration. The use of direct plasma in this study can further increase the degree of crystallization because of the close proximity of the substrate. The researchers disclosed that the amount of Y<sub>2</sub>O<sub>3</sub> doping in the thin-film electrolytes has significantly impacted fuel cell performance (as shown in Fig. 7g). The findings of this study suggest that the Y<sub>2</sub>O<sub>3</sub>

doping level of the YSZ thin-film electrolyte has a significant impact on electrochemical polarization processes to influence the fuel cell performance.

Recent research has shown that combining an ion conductor with electrode material is an efficient way to get high ion conductivity and has significant promise in electrolyte applications for intermediate temperature solid oxide fuel cell (LT-SOFCs) applications. According to Lee and colleagues (2005), YSZ-SrTiO<sub>3</sub> electrolyte improved ionic conductivity by up to two orders of magnitude over YSZ electrolyte. In a research study, Nie and his colleagues (2021) developed a new LaNiO<sub>3</sub>-YSZ composite electrolyte, which demonstrated an excellent peak power density of 399 mW cm<sup>-2</sup> at 450 °C and 1045 mW cm<sup>-2</sup> at 600 °C in H<sub>2</sub>/air atmosphere, as shown in Fig. 8b. The cells have high open-circuit voltages ranging from 0.946 to 1.134 V, which are near to theoretical values, as shown in Fig. 8a. Furthermore, the amount of LaNiO<sub>3</sub> in the YSZ-SrTiO<sub>3</sub> composite electrolyte affects the power density of these cells significantly. Selecting an appropriate cathode could be a viable way to increase the performance of the fuel cell. This study shows how to achieve high ionic conductivity using unique cathode-ion conductor composite materials.

Reducing ion-conducting resistance of the electrolyte material is essential for the development of low-temperature solid oxide fuel cells. This can be accomplished by using better ionic conductivity electrolyte materials or lowering the electrolyte thickness. Several researchers have used atomic layer deposition (ALD), pulsed laser deposition (PLD), and solution coating techniques to construct thin-film electrolytes (Huang et al. 2007; Shim et al. 2007; Oh et al. 2012). In a research study, plasma-enhanced atomic layer deposition (PEALD) was used to produce a thin film (nanoscale) yttria-stabilized zirconia (YSZ) electrolyte coating over a porous anodic aluminum oxide supporting substrate for solid oxide fuel cells (Ji et al. 2015). This research found that plasma-enhanced atomic layer deposition (PEALD) is an excellent method for depositing thin-film electrolytes on porous anodic aluminum oxide substrates because it allows for a significant reduction in film thickness and ohmic loss during electronic insulation and maintaining gas tightness. The SOFC-based thin film YSZ electrolyte (thickness of ~70 nm) produced a high open-circuit voltage (OCV) of ~1.17 V. Atomic force microscopy (AFM) was used to examine the grain size of PEALD-YSZ thin films formed on a silicon substrate (Fig. 9a). Figure 9b shows high-resolution transmission electron microscopy (TEM) images of the anodic aluminum oxide (AAO)-supported SOFC with 70-nm-thick PEALD-YSZ electrolyte, 320-nm-thick Pt anode, and 150-nm-thick porous Pt cathode. Polarization curves for micro-SOFCs with PEALD-YSZ electrolyte thicknesses of 70 and 210 nm were measured at 500 °C. In terms of peak power density, the cell with a 70-nm-thick electrolyte

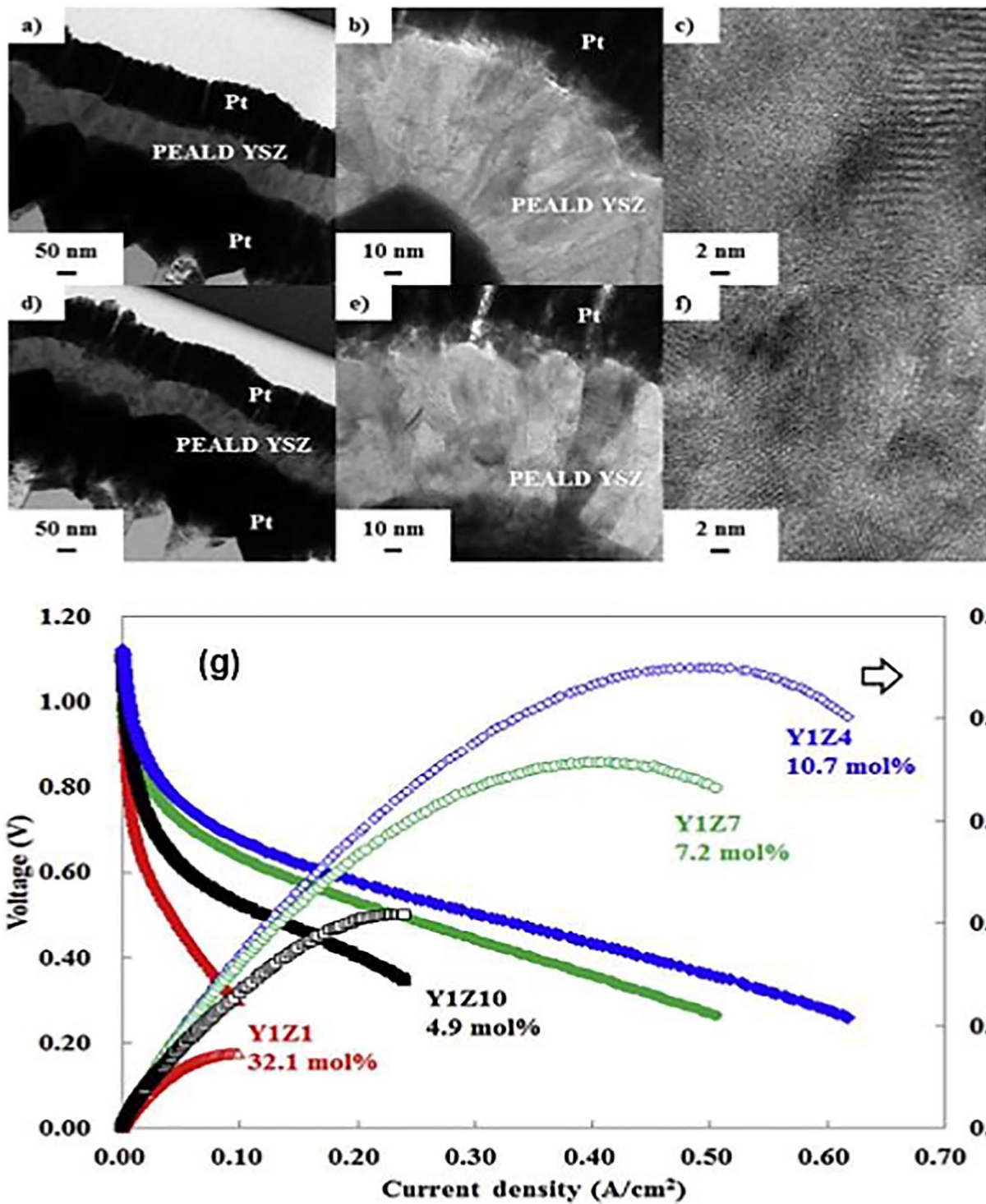
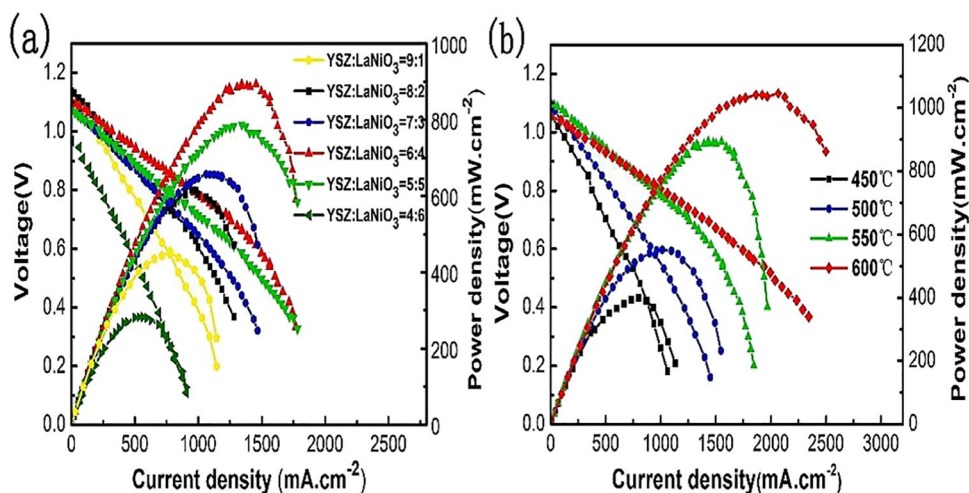


**Fig. 7** TEM images of microstructure of Y1Z1 and Y1Z4 thin film SOFC units, **a** microstructure of Y1Z1 fuel cell, **b** Y1Z1 cell thin film electrolyte, **c** TEM image of Y1Z1 electrolyte, **d** TEM picture of the microstructure of Y1Z4 fuel cell unit, **e** TEM image of Y1Z4 electrolyte, **f** TEM image of Y1Z4 electrolyte, **g** polarization curves

of SOFCs with YSZ electrolytes of various doping ratios measured at 450 °C, where the concentrations of Y<sub>2</sub>O<sub>3</sub> in Y1Z1, Y1Z4, Y1Z7, and Y1Z10 are 32.1 mol%, 10.7 mol%, 7.2 mol%, and 4.9 mol%, respectively (Cho et al. 2019). Reproduced with permission from the ref. (Cho et al. 2019). Copyright 2019 Elsevier



**Fig. 8** **a** Performance of fuel cell based on LaNiO<sub>3</sub>-YSZ electrolyte at 550 °C with various compositions, **b** performance of fuel cell based on 40LaNiO<sub>3</sub>-60YSZ electrolyte at different temperatures in H<sub>2</sub>/air atmosphere (Nie et al. 2021). Reproduced with permission from the ref. (Nie et al. 2021). Copyright 2021 Elsevier



outperformed the one with a 210-nm-thick electrolyte, as shown in Fig. 9c. The ohmic loss of the cell with PEALD-YSZ electrolyte is shown in Fig. 9d. The results indicated that reducing electrolyte thickness can reduce ohmic loss, which has significantly increased fuel cell performance.

### Ceria-based electrolyte used in fuel cells

Pure CeO<sub>2</sub> has a cubic fluorite structure at room temperature and is a poor oxygen ion conductor. An appreciable conductivity level can be achieved by doping of ceria, enabling doped ceria to be utilized as electrolyte material in SOFC (Qiao et al. 2018; Shin et al. 2019). However, at low partial pressure (< 10–15 atm.) and high temperature (around 700 °C), Ce<sup>4+</sup> present in ceria tends to reduce to Ce<sup>3+</sup> and form more oxygen vacancy and electrons, which are localized as polarons on Ce<sup>3+</sup> sites. Thus, the electronic hopping mechanism between Ce<sup>3+</sup> and Ce<sup>4+</sup> ions gives rise to *n*-type electronic conductivity, which leads to a drop in the open circuit voltage of SOFC. This larger ionic size of Ce<sup>3+</sup> than Ce<sup>4+</sup> hinders the migration of O<sup>2-</sup> ions and lowers the ionic conductivity. These reasons limit the use of CeO<sub>2</sub> as an electrolyte in the intermediate temperature range (500–700 °C) in SOFC (Shah et al. 2020; Hwang et al. 2021). Ceria-based electrolytes are considered good SOFC electrolytes. It has high electrode compatibility. Doped ceria shows high oxygen ion conductivity, particularly at a lower temperature as compared to stabilized zirconia. At intermediate temperatures, gadolinium and samarium-doped ceria were found to be good oxygen ion conductors. Arai and co-workers (Yahiro et al. 1988) investigated the consequence of doping of MgO, BaO, CaO, and MgO in ceria. The addition of strontium oxide and calcium oxide to ceria improves its ionic conductivity. When compared to strontium oxide and calcium oxide, adding magnesium oxide and barium oxide does not

significantly improve ionic conductivity due to the high size mismatch of Mg<sup>2+</sup> and Ba<sup>2+</sup> with Ce<sup>4+</sup> (Ng et al. 2016; Azim Jais et al. 2017).

Ceria-based electrolytes are widely explored as SOFC electrolytes because of their high electrode compatibility with oxygen ion conductivity, particularly at a lower temperature as compared to stabilized zirconia. However, pure CeO<sub>2</sub> possesses a cubic fluorite structure from room temperature to its melting point. Stoichiometric ceria is not a good ionic conductor. On doping ceria with acceptor metal oxides such as Gd<sub>2</sub>O<sub>3</sub>, Sm<sub>2</sub>O<sub>3</sub>, CaO, and SrO, an appreciable conductivity level can be achieved, enabling doped ceria to be utilized as electrolyte material in SOFC (Qiao et al. 2018; Shin et al. 2019). The effect of MgO, BaO, CaO, SrO, and MgO doping in ceria was fully explored in a research study. It has been observed that oxygen ion conductivity of ceria was improved significantly by the addition of SrO and CaO (Yahiro et al. 1988). Adding magnesium oxide and barium oxide does not considerably improve oxygen ion conductivity. The finding could be explained by the fact of large-size mismatch of Mg<sup>2+</sup> and Ba<sup>2+</sup> ions with Ce<sup>4+</sup> ion. Lowering the operating temperature can lower operation and manufacturing costs while also improving efficiency and long-term stability. Developing high oxygen ion conductive electrolytes is essential for attaining high power density at low temperatures. Despite the excellent ionic conductivity of doped ceria, ceria-based electrolytes have several drawbacks when used at intermediate temperatures. At high temperatures (around 700 °C), Ce<sup>4+</sup> in ceria tends to reduce to Ce<sup>3+</sup> and form more oxygen vacancy and electrons. Thus, the electronic hopping mechanism between Ce<sup>3+</sup> and Ce<sup>4+</sup> ions gives rise to *n*-type electronic conductivity, leading to a drop in the open-circuit voltage of SOFC. This larger ionic size of Ce<sup>3+</sup> than Ce<sup>4+</sup> hinders the migration of O<sup>2-</sup> ions and lowers the ionic conductivity. Meanwhile, the chemical



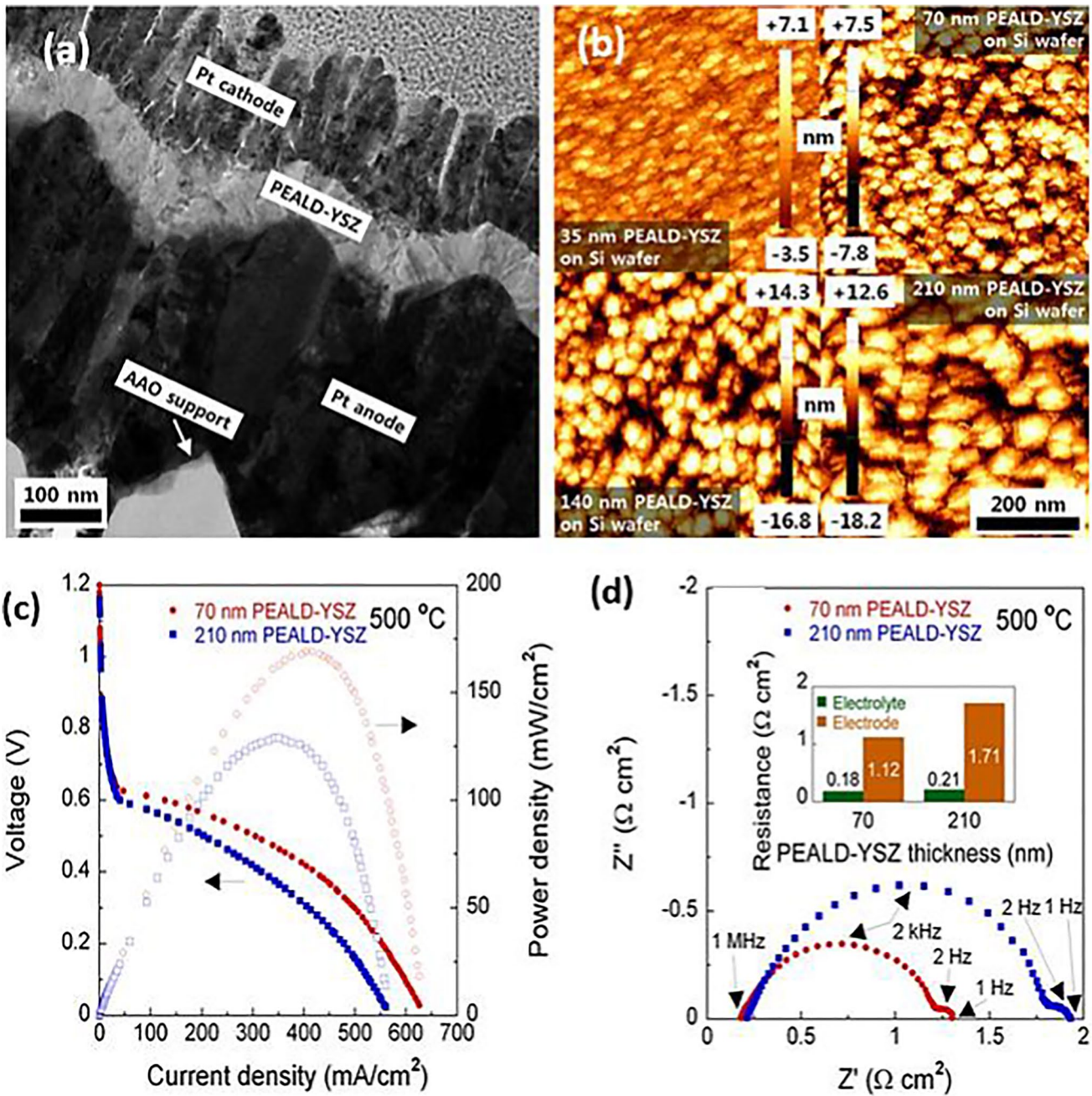


**Fig. 9** **a** TEM image of an AAO substrate-supported cell comprising 70-nm YSZ electrolyte, 150-nm Pt cathode, and 320-nm Pt anode, **b** AFM images of YSZ films with thicknesses of 35, 70, 140, and 210 nm deposited on flat silicon substrates (Ji et al. 2015). **c** Polari-

zation curves of the fuel cell made of REALD-YSZ electrolyte and **d** impedance data for cells with 70- and 210-nm-thick PEALD-YSZ electrolyte at 500 °C (Ji et al. 2015). Reproduced from the reference (Ji et al. 2015). Copyright 2015ACS

instability of  $Ce^{4+}$  under reduced atmospheres would result in mechanical failure. Lowering the operating temperature can lower operation and manufacturing costs while also improving efficiency and long-term stability. Developing high oxygen ion conductive electrolytes is essential for attaining high power density at low temperatures. Doped ceria (e.g.,  $Ce_{0.9}Gd_{0.1}O_2$ ,  $Ce_{0.8}Sm_{0.2}O_2$ ) have a very high

ionic conductivity and are commonly utilized as electrolyte materials for low-temperature solid oxide fuel cells (SOFCs) (Xia and Liu 2001; Zhang et al. 2006; Lee et al. 2014). However, internal short circuit behavior in doped ceria-based electrolytes makes it impractical to employ in operating conditions. The internal short circuit would result in a large drop in open-circuit voltage (OCV) and,

as a result, reduced SOFC operational efficiency (Zhang et al. 2007; Sun and Liu 2012).

Various techniques were developed to take advantage of doped ceria's high oxygen ion conductivity while avoiding the abovementioned limitations. A typical approach is to use the yttria-stabilized zirconia (YSZ) electron-blocking layer between the electrolyte membrane and anode support (Virkar 1991; Matsuda et al. 2007). The fuel cell performance reduces significantly due to the low oxygen ion conductivity of YSZ and the interaction between doped ceria and YSZ during sintering, despite the fact that the OCV is increased substantially (Price et al. 2005; Lim and Virkar 2009; Qian et al. 2013). Although the doped ceria electrolyte has a better conductivity at low temperatures than YSZ, with a conductivity of 0.019 to 0.011 S/cm at 600–500 °C (Fuentes and Baker 2009), electrolyte conductivity of about 0.01 S/cm is insufficient for building highly efficient low-temperature SOFCs (LTSOFCs). However, the ionic conductivity of these electrolytes at intermediate temperatures is insufficient for most technical applications, necessitating the search for ways to increase it. As a result, novel ways either to increase the conductivity of existing materials or develop new electrolyte materials are required for their realistic application in intermediate temperature. These reasons limit the use of  $\text{CeO}_2$  as an electrolyte in the intermediate temperature range (500–700 °C) in SOFCs (Shah et al. 2020; Hwang et al. 2021). Various techniques were developed to take advantage of doped ceria's high oxygen ion conductivity while avoiding limitations. A typical approach is to use the YSZ electron-blocking layer between the electrolyte membrane and anode support (Virkar 1991; Matsuda et al. 2007). However, the fuel cell performance reduces significantly due to the low oxygen ion conductivity of YSZ and the interaction between doped ceria and YSZ during sintering, even though the OCV is increased substantially (Price et al. 2005; Lim and Virkar 2009; Qian et al. 2013).

Few recent studies have reported that replacing ceria-Ni-based composite anode with  $\text{BaCeO}_3$ -Ni based composite anode in doped ceria electrolyte-based SOFCs is a more effective and realistic option to achieve high OCV (Liu et al. 2012; Sun and Liu 2012; Sun et al. 2014; Cao et al. 2015). This method uses Ba ion diffusion to react with doped ceria electrolyte in situ during the sintering process, forming an electron-blocking interlayer. For example, SOFC was created and evaluated in a research study employing a barium-containing anode and  $\text{Ce}_{0.8}\text{Sm}_{0.2}\text{O}_{2-\delta}$ -based electrolyte (Sun and Liu 2012). A thin  $\text{BaO-CeO}_2\text{-Sm}_2\text{O}_3$  composite interlayer is formed at high temperatures (Fig. 10a–b). The electron-blocking interlayer entirely eliminates the well-known internal short circuit in the doped ceria-based electrolyte (SDC) membrane. Except for the electron-blocking interlayer, the doped ceria electrolyte co-fired at 1150 °C was considerably porous. The dense electron-blocking interlayer created a

sufficient barrier for gas leakage, which facilitated the generation of high OCV. The diffusion of Ba from the anode to the SDC electrolyte membrane was confirmed by the SEM–EDS picture (Fig. 10b). However, the electrochemical performance of the cell was not improved considerably, especially at low temperatures. For doped ceria-based SOFCs, the cause of poor electrochemical performance could be that the catalytic performance of  $\text{BaCeO}_3$ -Ni-based anode is inferior than  $\text{CeO}_2$ -Ni-based anode. The catalytic ability and the microstructure of the electrodes have been shown to be highly associated with power performance. Additionally, the electrodes formed a strong bond with the electrolyte, indicating good compatibility. The cell (cell-improved, i.e., the cell containing dense electron-blocking interlayer) showed good power densities at intermediate temperature (600–700 °C) as shown in Fig. 10c. In contrast, a typical SDC-based cell (cell-unimproved) showed comparatively lower power densities at similar experimental conditions as shown in Fig. 10d. The significantly improved OCV values of cell-improved are responsible for the better improvement in cell function. Furthermore, the relationship between the thickness of the Ba-containing layer and cell performance, including OCV and power, is still unknown.

For doped ceria-based SOFCs, one effective and feasible choice to achieve high OCVs is using  $\text{BaCeO}_3$ -Ni composite as the anode. Ba ions diffuse from the anode during the sintering process and react with doped ceria electrolyte in situ, generating an electron-blocking interlayer. However, the electrochemical performance is inferior to doped ceria-based cells. The finding can be explained by the fact that the catalytic performance of doped  $\text{BaCeO}_3$ -Ni composite may be inferior to that of doped  $\text{CeO}_2$ -Ni anode. The microstructure of the electrodes and the catalytic characteristics is closely correlated with power performance. There is a need to investigate the relationship between cell performance and the thickness of the Ba-containing layer, particularly power output and OCV. For fuel cell applications,  $\text{Ce}_{0.8}\text{Sm}_{0.2}\text{O}_2$  (SDC) electrolyte and Ni- $\text{BaZr}_{0.1}\text{Ce}_{0.7}\text{Y}_{0.2}\text{O}_3$  (Ni-BZCY)-based bilayer anode was developed (Gong et al. 2016). During sintering, the anode layer aids in the formation of an electron blocking layer. The thickness of Ni-BZCY showed a big impact on the cell's electrochemical performance. The excellent power density was observed with a 50  $\mu\text{m}$  thickness of the Ni-BZCY layer (as shown in Fig. 11a). NiO-BZCY layer thickness showed a strong influence on the power density of the cells and OCVs. The single-cell showed good fuel cell performance in terms of power density and current density, as shown in Fig. 11b. Figure 11c and d shows that the single-cell has good performance stability with no performance decline in both open circuit and working conditions, demonstrating that the cell has a robust structure for long-term practical use.



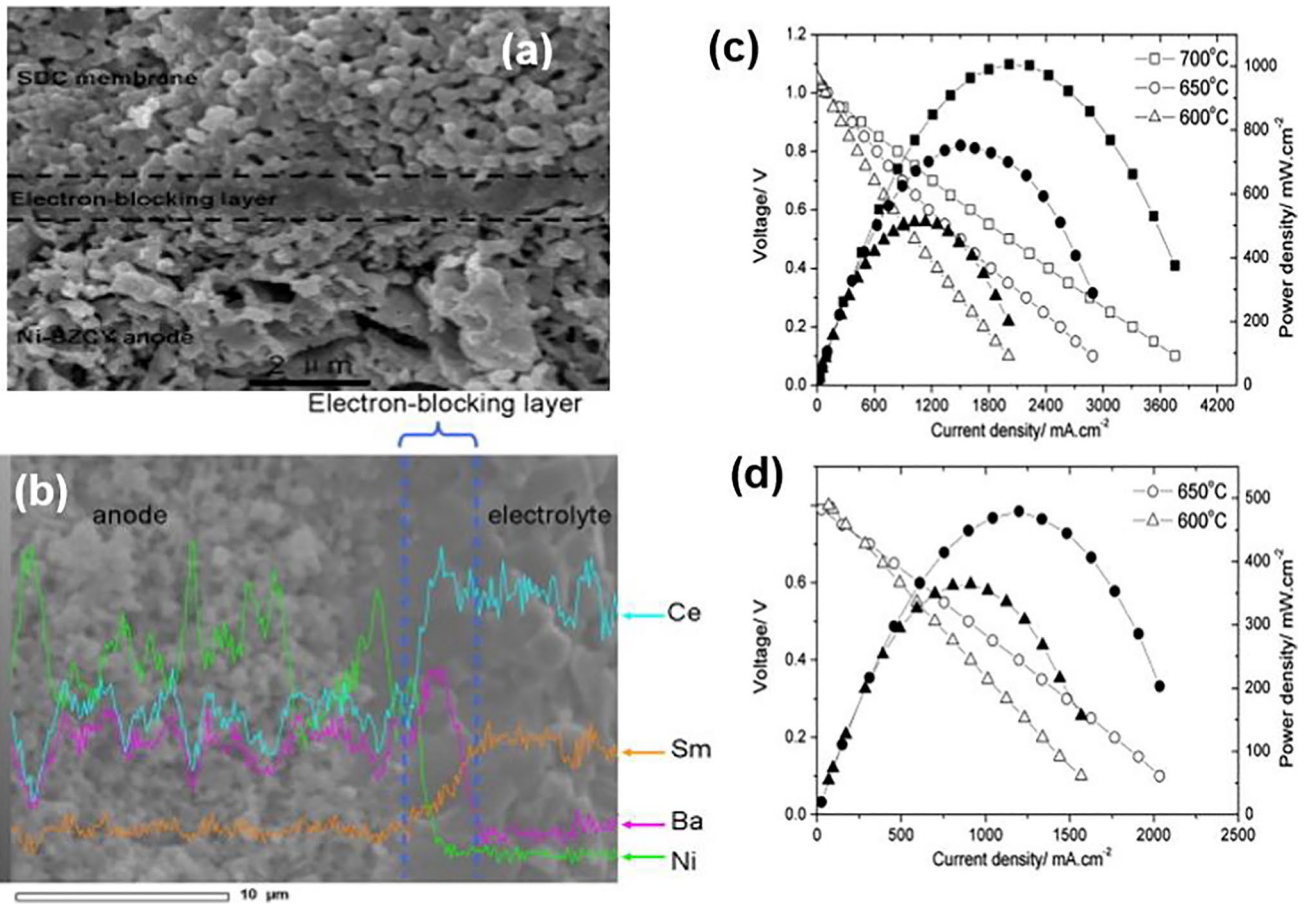
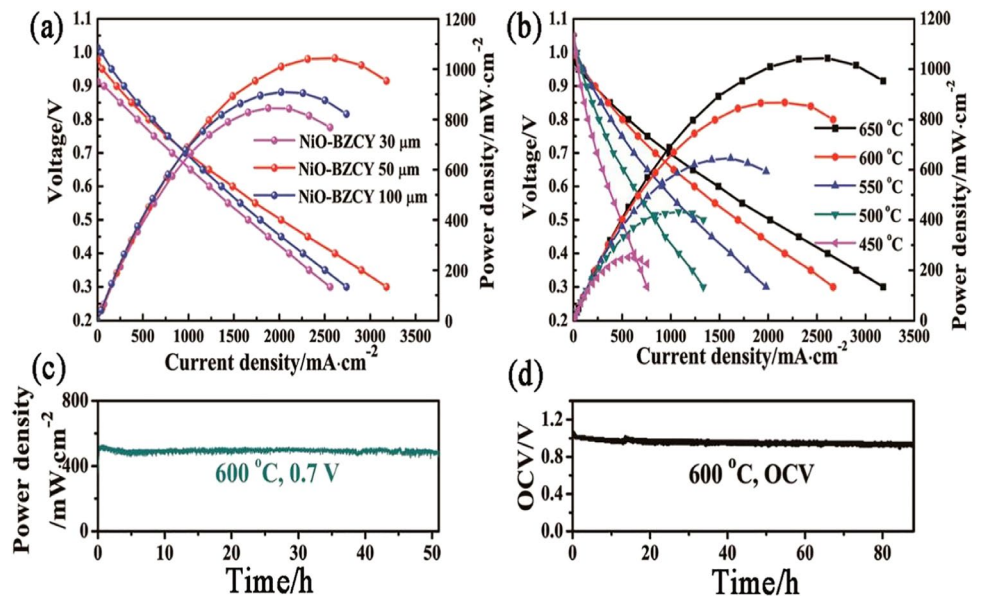


**Fig. 10** **a** The SEM picture of the cross section of the single-cell, **b** SEM-EDS analysis image of the anode/electrolyte interface, **c** fuel cell performance test of the cell-improved, **d** power density and I–V

curves of fuel cell with SDC (cell-unimproved) (Sun and Liu 2012). Adopted with permission from the ref. (Sun and Liu 2012). Copyright 2012 Elsevier

**Fig. 11** **a** Single-cell performance of NiO-BZCY at 650 °C, **b** single-cell performance of NiO-BZCY with a 50 μm thickness, **c** power density as a function of time, **d** stability of OCV tested under open conditions (Gong et al. 2016). Reproduced with permission from the ref. (Gong et al. 2016). Copyright 2016 ACS



Despite the fact that building highly efficient ceria-based SOFCs is a major challenge for commercial applications, various significant attempts are being made to develop viable SOFCs. For example, in one work, a bilayered anode consisting of Ni-BaZr<sub>0.1</sub>Ce<sub>0.7</sub>Y<sub>0.2</sub>O<sub>3-δ</sub> (Ni-BZCY) and Ni-Ce<sub>0.8</sub>Sm<sub>0.2</sub>O<sub>2-δ</sub> (Ni-SDC) and a doped ceria-based electrolyte (Ce<sub>0.8</sub>Sm<sub>0.2</sub>O<sub>2-δ</sub>) (SDC) was used to construct a novel form of SOFC (Gong et al. 2016). The Ni-BZCY functional layer provided a Ba source for creating an electron-blocking layer at the interface of electrolyte and anode during sintering and catalysis activity. The diffusion of components at the electrolyte-anode interface to form an electron-blocking layer was confirmed in Fig. 12a. The thickness of the Ni-BZCY layer showed a big impact on the electron-blocking layer's characteristics and the cell's electrochemical performance. The OCVs of the cells have been found to be directly connected to the thickness of the electron-blocking layer, and a thick electron-blocking layer is required to completely remove the internal short circuit. Figure 12b shows the OCVs of the different cells. The cell showed excellent fuel

cell performance in terms of OCV and peak power density (1068 mW cm<sup>-2</sup>) with 50-μm-thick Ni-BZCY layer at 650 °C as illustrated in Fig. 12c. The results of this study showed that the cell has a noticeable advantage in terms of producing high-power low temperatures. Figure 12d shows that the cell has good stability and nearly no performance decline in both working and open circuit conditions, showing that the cell has a robust structure for long-term practical use.

A potential strategy for developing electrolytes for low-temperature solid oxide fuel cells (LT-SOFCs) is to build nanocomposite electrolyte materials utilizing both ceria and bismuth oxide. In a recent study, ceria-embedded gadolinium-stabilized bismuth oxide was used to make a nanocomposite solid electrolyte for LT-SOFC applications (Parbin and Rafiuddin 2022). A solid-state technique was used to synthesize several compositions with the formula (1 - x)Bi<sub>2</sub>O<sub>3</sub>-Gd<sub>2</sub>O<sub>3</sub>:xCeO<sub>2</sub> (GDBC). SEM and TEM techniques were used to examine the morphology of the solid electrolyte samples. Typical SEM images of Bi<sub>2</sub>O<sub>3</sub>, CeO<sub>2</sub>, Gd<sub>2</sub>O<sub>3</sub>, Bi<sub>2</sub>O<sub>3</sub>-Gd<sub>2</sub>O<sub>3</sub>-CeO<sub>2</sub> (GDBC),

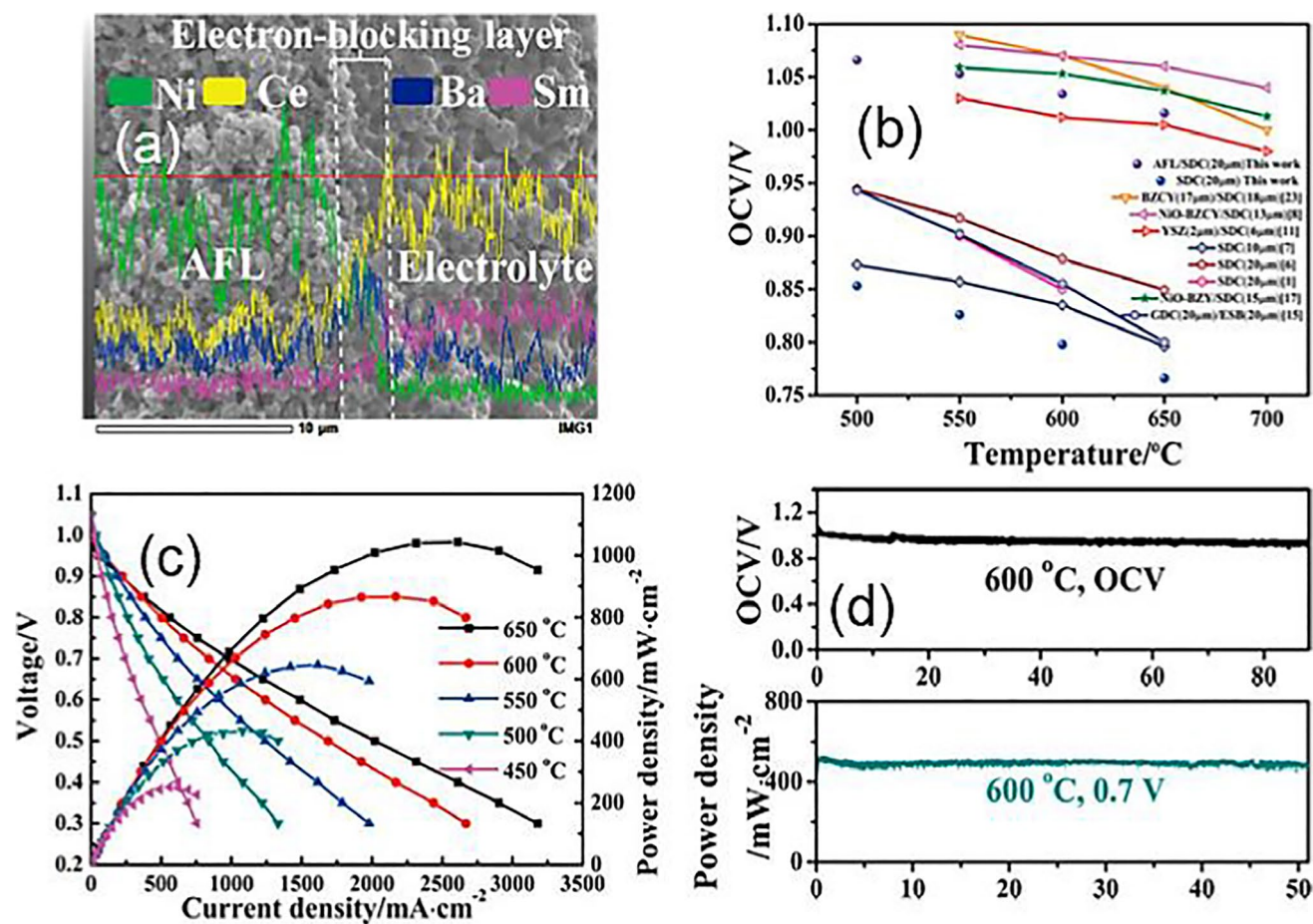


**Fig. 12** **a** SEM-EDS analysis of the interface between anode functional layer and SDC electrolyte sintered at 1350 °C, **b** OCV values of various doped ceria (DCO)-based SOFCs, **c** polarization curves of

the single-cell, **d** power density and short-term stability of OCV as a function of time. Reproduced from the reference (Gong et al. 2016). Copyright ACS 2020



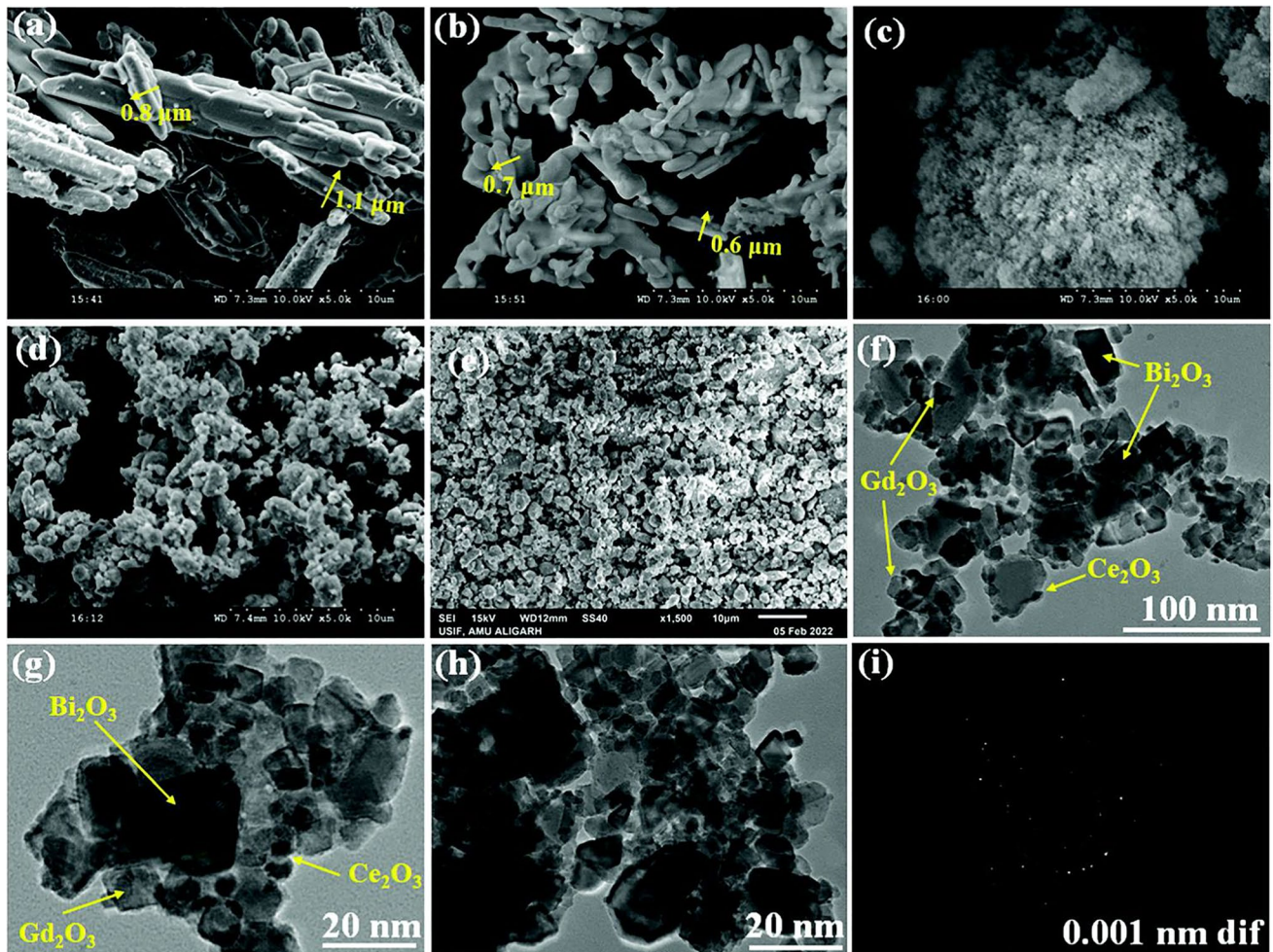


**Fig. 13** SEM images of **a**  $\text{Bi}_2\text{O}_3$ , **b**  $\text{Gd}_2\text{O}_3$ , **c**  $\text{CeO}_2$ , **d**  $\text{Bi}_2\text{O}_3$ – $\text{Gd}_2\text{O}_3$ , **e**  $60\text{Bi}_2\text{O}_3$ – $\text{Gd}_2\text{O}_3$ : $40\text{CeO}_2$ . **f–h** TEM images of  $60\text{Bi}_2\text{O}_3$ – $\text{Gd}_2\text{O}_3$ : $40\text{CeO}_2$  nanocomposite electrolyte, **i** SAED pattern of

$60\text{Bi}_2\text{O}_3$ – $\text{Gd}_2\text{O}_3$ : $40\text{CeO}_2$  nanocomposite electrolyte (Parbin and Rafiuddin 2022). Adopted with permission from the ref. (Parbin and Rafiuddin 2022). Copyright RSC under common creative license

and  $\text{Bi}_2\text{O}_3$ – $\text{Gd}_2\text{O}_3$  (GDB) are shown in Fig. 13a–e. The doped materials ( $\text{Gd}_2\text{O}_3$  and  $\text{CeO}_2$ ) are clearly embedded in the  $\text{Bi}_2\text{O}_3$  matrix, as shown by the surface morphology of  $60\text{Bi}_2\text{O}_3$ – $\text{Gd}_2\text{O}_3$ : $40\text{CeO}_2$ . TEM was used to explore the structural properties of GDBC nanocomposite solid electrolytes. Figure 13f–h shows the embedded  $\text{CeO}_2$  nanoparticles on the surface of  $\text{Bi}_2\text{O}_3$ – $\text{Gd}_2\text{O}_3$ , which are in contact with one another, as seen in TEM images of a 40 wt%  $\text{CeO}_2$  nanocomposite solid electrolyte. In addition, the polycrystalline structure of the nanocomposite electrolyte is indicated in Fig. 13i. By providing additional oxygen-ion conduction channels inside the parent network,  $\text{CeO}_2$  nanofillers increased ionic conductivity. GDBC showed good conductivity at low temperatures. Material conductivity and production costs are the issues for the commercialization of LT-SOFCs. Hence, this nanocomposite solid electrolyte with 40%  $\text{CeO}_2$  could be a good choice for fabricating electrolytes for fuel cell

applications due to its high ionic conductivity at low temperatures and low cost. SEM and TEM techniques were used to examine the morphology of the solid electrolyte samples. Typical SEM images of  $\text{Bi}_2\text{O}_3$ ,  $\text{CeO}_2$ ,  $\text{Gd}_2\text{O}_3$ ,  $\text{Bi}_2\text{O}_3$ – $\text{Gd}_2\text{O}_3$ – $\text{CeO}_2$  (GDBC), and  $\text{Bi}_2\text{O}_3$ – $\text{Gd}_2\text{O}_3$  (GDB) are shown in Fig. 13a–e. The doped materials ( $\text{Gd}_2\text{O}_3$  and  $\text{CeO}_2$ ) are clearly embedded in the  $\text{Bi}_2\text{O}_3$  matrix, as shown by the surface morphology of  $60\text{Bi}_2\text{O}_3$ – $\text{Gd}_2\text{O}_3$ : $40\text{CeO}_2$ . The structural features of GDBC nanocomposite solid electrolyte with 40%  $\text{CeO}_2$  were investigated using TEM to confirm the production of nanocomposite material. Figure 13f–h shows the embedded  $\text{CeO}_2$  nanoparticles on the surface of  $\text{Bi}_2\text{O}_3$ – $\text{Gd}_2\text{O}_3$ , which are in contact with one another, as seen in TEM images of a 40 wt%  $\text{CeO}_2$  nanocomposite solid electrolyte.

## Other solid oxide electrolytes for SOFCs

Bismuth oxide exhibits two crystallographic polymorphisms, i.e.,  $\alpha$ - $\text{Bi}_2\text{O}_3$  and  $\delta$ - $\text{Bi}_2\text{O}_3$ . Below 730 °C,  $\alpha$ - $\text{Bi}_2\text{O}_3$  is a stable form which possesses a monoclinic structure and  $\delta$ - $\text{Bi}_2\text{O}_3$ , which is stable above 730 °C up to its melting temperature of 825 °C, possesses a cubic structure (Ari et al. 2018; Masina et al. 2021).  $\delta$ - $\text{Bi}_2\text{O}_3$  has a defect fluorite structure in which 25% of sites in the oxygen sublattice are vacant. This high concentration of intrinsic defect renders high ionic conductivity to this (Ermiş 2019; Liang and Chou 2020). Thus, in the pure form of  $\text{Bi}_2\text{O}_3$ , its useful temperature range is very narrow, which is 730 to 825 °C. The high-temperature  $\delta$ -phase can be stabilized to lower temperature by the addition of various rare earth oxides like  $\text{Nb}_2\text{O}_5$ ,  $\text{Ta}_2\text{O}_5$ ,  $\text{WO}_3$ , and  $\text{Y}_2\text{O}_3$  (Lunca Popa et al. 2017; Orozco-Hernández et al. 2020). However, in phase-stabilized bismuth oxide, an order–disorder transition of oxygen sublattice occurs around 600 °C with aging, which leads to decay in conductivity (Jiang et al. 2002; Joh et al. 2017). Besides, the main problem associated with stabilized  $\text{Bi}_2\text{O}_3$ -based materials is their ease of reduction at low oxygen partial pressure ( $P_{\text{O}_2} < 10$ –13 atmosphere at 600 °C) conditions. In addition to this, the volatile nature of  $\text{Bi}_2\text{O}_3$  at moderate temperature ( $\sim 700$  °C) and poor mechanical strength (bending strength 80 MPa) restrict their practical use as SOFC electrolyte material (Takahashi et al. 1977; Jiang et al. 2002; He et al. 2018).

Sr and Mg-doped  $\text{LaGaO}_3$  (LSGM)-based electrolytes have recently been widely investigated for SOFC applications because of their strong ionic conductivity at low temperatures and low electronic conductivity (He et al. 2018). It appears to be the leading new generation material for use as a solid electrolyte in SOFCs operating at  $\sim 800$  °C due to its outstanding chemical and electrical properties (ionic conductivity  $\sim 0.10$  S/cm at 800 °C). However, the synthesis of LSGM without a second phase was found to be difficult; secondary phases such as  $\text{LaSrGa}_3\text{O}_7$ ,  $\text{LaSrGaO}_4$ ,  $\text{La}_4\text{Ga}_2\text{O}_9$ , and  $\text{LaGa}_2\text{O}_4$  were formed easily (Jiang et al. 2002). If the LSGM is made of cubic perovskite, it shows a higher ionic conductivity; however, if secondary phases occur, the ionic conductivity of the LSGM drops substantially. However, thorough research into the microstructures of this material, particularly the effect of chemical compositions on the microstructure, may be able to resolve these issues and give a better foundation for using LSGM in SOFCs. However, LSGM is significantly more expensive than ceria-based electrolytes, and electrode materials made of LSGM have been reported to have durability issues (Ari et al. 2018).

Because of the high activation energy of oxygen ion conduction, the conductivity of oxygen ions in ceramic

electrolytes often reduces rapidly as the operating temperature declines. As a result, proton-conducting solid oxide materials are more appropriate as intermediate and low temperature electrolytes than oxygen ion-conducting solid oxide electrolytes. The vehicle mechanism and the Grotthuss method are the two basic proton transport mechanisms for proton-conducting electrolytes (Cao et al. 2021). A proton joins an oxygen ion to produce hydroxide ion ( $\text{OH}^-$ ), which moves through oxygen vacancies in the vehicle mechanism. The Grotthuss mechanism is a two-step process that involves the formation of a hydroxide ion and proton transfer between nearby oxygen ions where the proton is the only movable species in the Grotthuss process, with oxygen confined to the area of its crystallographic location. In the 1980s, it was observed for the first time that  $\text{SrZrO}_3$ -based materials can conduct protons. In another study, Iwahara and co-workers (1981) observed that doped  $\text{SrCeO}_3$  could exhibit proton conductivity when exposed to a hydrogen-based environment. However,  $\text{SrCeO}_3$ -based materials often have limited proton conductivity and poor chemical stability, resulting in the formation of  $\text{SrCO}_3$  and  $\text{CeO}_2$  at high temperatures in a  $\text{CO}_2$  atmosphere. Then, different research groups investigated the characteristics of high-temperature proton-conducting materials based on doped  $\text{BaCeO}_3$  (Hibino et al. 1992; Ma et al. 1999; Danilov et al. 2018). Since then, researchers from academics and industries have focused their attention on this type of proton-conducting electrolyte material. Many protonic ceramics, including  $\text{ABO}_3$  simple perovskite and  $\text{A}_2\text{B}_2\text{O}_5$  brownmillerite, have been created to date. Among proton-conducting electrolyte materials, the  $\text{ABO}_3$  simple perovskite is the most popular proton-conducting electrolyte material because its crystal structure promotes proton mobility. Doped  $\text{BaZrO}_3$  and  $\text{BaCeO}_3$  are two forms of proton-conducting electrolytes that are promising. Oxygen vacancies are generated by replacing the B-site ions of  $\text{BaZrO}_3$  and  $\text{BaCeO}_3$  with dopants such as the Y ion, which helps produce protonic defects by dissociative adsorption of water. A good metal oxide electrolyte material should have three characteristics: high ionic conductivity, sinterability, chemical stability, and thermal stability.  $\text{BaCeO}_3$ -based electrolytes have higher proton conductivity (greater than 0.01 S/cm) (Rajendran et al. 2021). As a result, doped  $\text{BaCeO}_3$  materials are among the most investigated proton conductors in recent times. Different rare earth elements have been partially doped in  $\text{BaCeO}_3$ 's B-site to improve proton conductivity and chemical and thermal stability (Wang et al. 2022). Because of their intrinsic basicity,  $\text{BaCeO}_3$ -based materials react fast with acidic gases to form  $\text{BaSO}_4$  and  $\text{BaCO}_3$ , which hinder proton migration and cause significant thermal expansion. Matsumoto and co-workers (Medvedev et al. 2014) studied the effects of various dopants such as  $\text{Tm}^{3+}$ ,



$\text{Lu}^{3+}$ ,  $\text{Y}^{3+}$ ,  $\text{Yb}^{3+}$ ,  $\text{Sc}^{3+}$ , and  $\text{In}^{3+}$  on the conductivity and stability of  $\text{BaCeO}_3$ . It was observed as the ionic radius of dopants increased, the ionic conductivity increased, but the chemical stability dropped. Among these doped oxides, the  $\text{Y}^{3+}$ -doped  $\text{BaCeO}_3$  (BCY) exhibited the best proton conductivity, whereas the  $\text{Sc}^{3+}$ -doped  $\text{BaCeO}_3$  showed the best chemical stability. Doped  $\text{BaZrO}_3$  is substantially more chemically stable than  $\text{BaCeO}_3$ -based compounds in acidic environments. On the other hand,  $\text{BaZrO}_3$ -based electrolytes confront a significant hurdle due to their inability to build a compact structure. Due to  $\text{BaZrO}_3$ 's poor sinterability, the samples usually have low density and high grain boundary resistance, resulting in low proton conductivity. However, the disadvantages of  $\text{BaZrO}_3$  can be mitigated by applying sintering aids and advanced thin-film fabrication processes. Proton conductivity is higher in  $\text{BaCeO}_3$ -based electrolytes, but chemical stability is poor (Sun and Liu 2012; Sun et al. 2014). On the other hand,  $\text{BaZrO}_3$ -based electrolytes have a low proton conductivity but high chemical stability. Among these doped oxides, the  $\text{Y}^{3+}$ -doped  $\text{BaCeO}_3$  (BCY) exhibited the best proton conductivity, whereas the  $\text{Sc}^{3+}$ -doped  $\text{BaCeO}_3$  showed the best chemical stability. Doped  $\text{BaZrO}_3$  is substantially more chemically stable than  $\text{BaCeO}_3$ -based compounds in acidic environments. On the other hand,  $\text{BaZrO}_3$ -based electrolytes confront a significant hurdle due to their inability to build a compact structure. Due to  $\text{BaZrO}_3$ 's poor sinterability, the samples usually have low density and high grain boundary resistance, resulting in low proton conductivity (Ma et al. 1999). However, the disadvantages of  $\text{BaZrO}_3$  can be mitigated by applying sintering aids and advanced thin-film fabrication processes. For proton conductor development, combining  $\text{BaZrO}_3$ -based oxide and  $\text{BaCeO}_3$  to generate novel  $\text{BaCe}_x\text{Zr}_{1-x}\text{O}_3$ -based electrolytes is a viable choice and  $\text{BaCe}_x\text{Zr}_{1-x}\text{O}_3$ -based electrolytes are widely studied. Under certain conditions,  $\text{BaCeO}_3$ -based electrolytes demonstrate oxygen ion conductivity as well as proton conductivity. The perovskite  $\text{BaZr}_{0.1}\text{Ce}_{0.7}\text{Y}_{0.1}\text{Yb}_{0.1}\text{O}_3$  (BZCYYb), composites based on  $\text{CeO}_2$  and carbonate are the most well-known dual ion electrolyte (Anwar et al. 2016; Danilov et al. 2018). Fuel cells with dual ion electrolytes have produced appealing power output at low temperatures and can combine the benefits of oxygen ion and proton conduction.

## Concluding remarks

Fuel cell technology is urgently needed as the next-generation energy conversion technology in order to produce clean and sustainable energy. Due to their superior ability to minimize air pollution, high fuel flexibility, and high energy conversion efficiency, SOFCs are considered the most ideal

fuel cell for generating electricity among all other fuel cells. For SOFC technology to be commercialized on large scale, a suitable electrolyte for SOFCs must be developed. In accordance with the former statement, the  $\text{CeO}_2$  and  $\text{ZrO}_2$ -based oxides are the electrolyte materials that have received the greatest attention for use in fuel cell technology as significant developments in the creation of sustainable and clean energy. Among various electrolyte materials, zirconia-based electrolytes have the great potential to be used as the electrolyte in SOFC due to their higher thermal stability, non-reducing nature, and higher mechanical strength, along with acceptable oxygen ion conductivity. However, zirconia-based electrolytes have poor ionic conductivity below  $850^\circ\text{C}$ , making them unsuitable for intermediate temperature working environments. On the other hand, ceria-based materials are being studied as electrolytes for intermediate SOFCs because of their good electrode compatibility and higher oxygen ion conductivity, particularly at lower temperatures. The development of electrolytes for solid oxide fuel cells that operate at low ( $400\text{--}650^\circ\text{C}$ ) and intermediate ( $650\text{--}850^\circ\text{C}$ ) temperatures has recently attracted the attention of numerous research teams. As far as the limitations are concerned, due to higher working temperatures of SOFCs which could be mitigated by substituting conventional electrolytes by some recently developed advanced electrolytes, which has proved to possess better ionic conductivity along with good chemical, thermal, and mechanical stability from low to intermediate temperatures. The most recent developments in zirconia- and ceria-based electrolyte materials have illustrated that there is considerable promise for using intermediate temperature SOFCs as an efficient approach for the next generation energy conversion technology.

**Acknowledgements** We acknowledge Mahatma Gandhi Central Library, IIT Roorkee, for providing all literature.

**Author contribution** Tushar Kanti Maiti: conceptualization, writing, reviewing, editing, visualization, data analysis. Jagannath Majhi: Editing, visualization. Subrata Kumar Maiti: conceptualization, reviewing. Jitendra Singh: conceptualization, editing. Prakhar Dixit: editing, visualization. Tushita Rohilla: reviewing, editing. Samaresh Ghosh: conceptualization, data analysis. Sakchi Bhushan: reviewing, visualization. Sujay Chattopadhyay: conceptualization, supervision.

**Funding** This work was financially supported by the Ministry of Human Resources Development, India, and IIT Roorkee, India.

**Data availability** Not applicable.

## Declarations

**Ethical approval** We have obtained all ethical approval.

**Consent to participate** All authors voluntarily agreed to participate in this study.

**Consent for publication** All authors have agreed to publish.

**Competing interests** The authors declare no competing interests.

## References

- Abdalla AM, Hossain S, Azad AT et al (2018) Nanomaterials for solid oxide fuel cells: a review. *Renew Sustain Energy Rev* 82:353–368. <https://doi.org/10.1016/j.rser.2017.09.046>
- Accardo G, Dell'aghi G, Frattini D et al (2017) Electrical behaviour and microstructural characterization of magnesia co-doped ScSZ nanopowders synthesized by urea co-precipitation. *Chem Eng Trans* 57:1345–1350. <https://doi.org/10.3303/CET1757225>
- Afroze S, Karim AH, Cheok Q et al (2019) Latest development of double perovskite electrode materials for solid oxide fuel cells: a review. *Front Energy* 13:770–797. <https://doi.org/10.1007/s11708-019-0651-x>
- Aguadero A, Fawcett L, Taub S et al (2012) Materials development for intermediate-temperature solid oxide electrochemical devices. *J Mater Sci* 47:3925–3948. <https://doi.org/10.1007/s10853-011-6213-1>
- Andújar JM, Segura F (2009) Fuel cells: History and updating. A walk along two centuries. *Renew Sustain Energy Rev* 13:2309–2322. <https://doi.org/10.1016/j.rser.2009.03.015>
- Anwar M, Muchtar A, Somalu MR (2016) Effects of various co-dopants and carbonates on the properties of doped ceria-based electrolytes: a brief review. *Int J Appl Eng Res* 11:9921–9928
- Arachi Y, Asai T, Yamamoto O et al (2001) Electrical conductivity of  $ZrO_2$ - $Sc_2O_3$  doped with  $HfO_2$ ,  $CeO_2$ , and  $Ga_2O_3$ . *J Electrochem Soc* 148:A520. <https://doi.org/10.1149/1.1366622>
- Arachi Y, Sakai H, Yamamoto O et al (1999) Electrical conductivity of the  $ZrO_2$ - $Ln_2O_3$  ( $Ln = \text{lanthanides}$ ) system. *Solid State Ion* 121:133–139. [https://doi.org/10.1016/S0167-2738\(98\)00540-2](https://doi.org/10.1016/S0167-2738(98)00540-2)
- Ari M, Balci M, Polat Y (2018) Synthesis and characterization of  $(Bi_2O_3)_{1-x-y-z}(Gd_2O_3)_x(Sm_2O_3)_y(Eu_2O_3)_z$  quaternary solid solutions for solid oxide fuel cell. *Chinese J Phys* 56:2958–2966. <https://doi.org/10.1016/j.cjph.2018.10.001>
- Azim Jais A, Muhammed Ali SA, Anwar M et al (2017) Enhanced ionic conductivity of scandia-ceria-stabilized-zirconia ( $10Sc1CeSZ$ ) electrolyte synthesized by the microwave-assisted glycine nitrate process. *Ceram Int* 43:8119–8125. <https://doi.org/10.1016/j.ceramint.2017.03.135>
- Badwal SPS (1992) Zirconia-based solid electrolytes: microstructure, stability and ionic conductivity. *Solid State Ion* 52:23–32. [https://doi.org/10.1016/0167-2738\(92\)90088-7](https://doi.org/10.1016/0167-2738(92)90088-7)
- Badwal SPS, Ciacchi FT (2000) Oxygen-ion conducting electrolyte materials for solid oxide fuel cells. *Ionics (kiel)* 6:1–21. <https://doi.org/10.1007/BF02375543>
- Badwal SPS, Ciacchi FT, Milosevic D (2000) Scandia-zirconia electrolytes for intermediate temperature solid oxide fuel cell operation. *Solid State Ion* 136–137:91–99. [https://doi.org/10.1016/S0167-2738\(00\)00356-8](https://doi.org/10.1016/S0167-2738(00)00356-8)
- Bhattacharyya R, Omar S (2018) Electrical conductivity study of B-site Ga doped non-stoichiometric sodium bismuth titanate ceramics. *J Alloys Compd* 746:54–61. <https://doi.org/10.1016/j.jallcom.2018.02.213>
- Cao J, Gong Z, Hou J et al (2015) Novel reduction-resistant  $Ba(Ce, Zr)_{1-x}Gd_xO_{3-\delta}$  electron-blocking layer for  $Gd_0.1Ce_0.9O_{2-\delta}$  electrolyte in IT-SOFCs. *Ceram Int* 41:6824–6830. <https://doi.org/10.1016/j.ceramint.2015.01.131>
- Cao J, Su C, Ji Y et al (2021) Recent advances and perspectives of fluorite and perovskite-based dual-ion conducting solid oxide fuel cells. *J Energy Chem* 57:406–427. <https://doi.org/10.1016/j.jechem.2020.09.010>
- Chao CC, Hsu CM, Cui Y, Prinz FB (2011) Improved solid oxide fuel cell performance with nanostructured electrolytes. *ACS Nano* 5:5692–5696. <https://doi.org/10.1021/nn201354p>
- Chen D, Xu Y, Tade MO, Shao Z (2017) General regulation of air flow distribution characteristics within planar solid oxide fuel cell stacks. *ACS Energy Lett* 2:319–326. <https://doi.org/10.1021/acseenergylett.6b00548>
- Chen G, Wang Y, Sunarso J et al (2016a) A new scandium and niobium co-doped cobalt-free perovskite cathode for intermediate-temperature solid oxide fuel cells. *Energy* 95:137–143. <https://doi.org/10.1016/j.energy.2015.11.061>
- Chen K, Li N, Ai N et al (2016b) Polarization-induced interface and Sr segregation of in situ assembled  $La_{0.6}Sr_{0.4}Co_{0.2}Fe_{0.8}O_{3-\delta}$  electrodes on  $Y_2O_3$ - $ZrO_2$  electrolyte of solid oxide fuel cells. *ACS Appl Mater Interfaces* 8:31729–31737. <https://doi.org/10.1021/acsami.6b11665>
- Chen Y, Gerdes K, Paredes Navia SA et al (2019) Conformal electrocatalytic surface nanoionics for accelerating higher-temperature electrochemical reactions in solid oxide fuel cells. *Nano Lett* 19:8767–8773. <https://doi.org/10.1021/acs.nanolett.9b03515>
- Cho GY, Lee YH, Yu W et al (2019) Optimization of  $Y_2O_3$  dopant concentration of yttria stabilized zirconia thin film electrolyte prepared by plasma enhanced atomic layer deposition for high performance thin film solid oxide fuel cells. *Energy* 173:436–442. <https://doi.org/10.1016/j.energy.2019.01.124>
- Dadashzadeh M, Ahmad A, Khan F (2016) Dispersion modelling and analysis of hydrogen fuel gas released in an enclosed area: a CFD-based approach. *Fuel* 184:192–201. <https://doi.org/10.1016/j.fuel.2016.07.008>
- Danilov NA, Lyagaeva JG, Medvedev DA et al (2018) Transport properties of highly dense proton-conducting  $BaCe_{0.8-x}Zr_xDy_{0.2}O_{3-\delta}$  materials in low- and high-temperature ranges. *Electrochim Acta* 284:551–559. <https://doi.org/10.1016/j.electacta.2018.07.179>
- Duan C, Tong J, Shang M, et al (2015) Readily processed protonic ceramic fuel cells with high performance at low temperatures. *Science* (80- ) 349:1321–1326. <https://doi.org/10.1126/science.aab3987>
- Eigenbrodt BC, Pomfret MB, Steinhurst DA et al (2011) Direct, in situ optical studies of Ni-YSZ anodes in solid oxide fuel cells operating with methanol and methane. *J Phys Chem C* 115:2895–2903. <https://doi.org/10.1021/jp109292r>
- Ermis İ (2019) Fabrication of  $Bi_{0.95-x}Er_{0.05}MxO_{1.5-\delta}$  ( $M = \text{Lu, Ho, and Gd}$ ) electrolyte for intermediate temperature solid oxide fuel cells. *J Aust Ceram Soc* 55:711–718. <https://doi.org/10.1007/s41779-018-0282-4>
- Fini D, Badwal SPS, Giddey S et al (2018) Evaluation of  $Sc_2O_3$ - $CeO_2$ - $ZrO_2$  electrolyte-based tubular fuel cells using activated charcoal and hydrogen fuels. *Electrochim Acta* 259:143–150. <https://doi.org/10.1016/j.electacta.2017.10.140>
- Fleischhauer F, Terner M, Bermejo R et al (2015) Fracture toughness and strength distribution at room temperature of zirconia tapes used for electrolyte supported solid oxide fuel cells. *J Power Sources* 275:217–226. <https://doi.org/10.1016/j.jpowsour.2014.10.083>
- Fu Q, Li Z, Wei W et al (2021) Performance degradation prediction of direct internal reforming solid oxide fuel cell due to Ni-particle coarsening in composite anode. *Energy Convers Manag* 233:113902. <https://doi.org/10.1016/j.enconman.2021.113902>
- Fuentes RO, Baker RT (2009) Structural, morphological and electrical properties of  $Gd_{0.1}Ce_{0.9}O_{1.95}$  prepared by a citrate



- complexation method. *J Power Sources* 186:268–277. <https://doi.org/10.1016/j.jpowsour.2008.09.119>
- Fujimori H, Yashima M, Kakihana M, Yoshimura M (1998) Structural changes of scandia-doped zirconia solid solutions: Rietveld analysis and Raman scattering. *J Am Ceram Soc* 81:2885–2893. <https://doi.org/10.1111/j.1151-2916.1998.tb02710.x>
- Ghezel-Ayagh H, Jolly S, Patel D, Stauffer D (2013) Solid oxide fuel cell system utilizing syngas from coal gasifiers. *Ind Eng Chem Res* 52:3112–3120. <https://doi.org/10.1021/ie300841m>
- Gong Z, Sun W, Shan D et al (2016) Tuning the thickness of Ba-containing “functional” Layer toward high-performance ceria-based solid oxide fuel cells. *ACS Appl Mater Interfaces* 8:10835–10840. <https://doi.org/10.1021/acsami.6b01000>
- Grimes P (2000) Historical pathways for fuel cells. The new electric century. *Proc Annu Batter Conf Appl Adv* 2000-January:41–45. <https://doi.org/10.1109/BCAA.2000.838369>
- Guan L, Le S, He S et al (2015) Densification behavior and space charge blocking effect of Bi<sub>2</sub>O<sub>3</sub> and Gd<sub>2</sub>O<sub>3</sub> Co-doped CeO<sub>2</sub> as electrolyte for solid oxide fuel cells. *Electrochim Acta* 161:129–136. <https://doi.org/10.1016/j.electacta.2015.02.090>
- Haering C, Roosen A, Schichl H, Schnöller M (2005) Degradation of the electrical conductivity in stabilised zirconia system Part II: scandia-stabilised zirconia. *Solid State Ion* 176:261–268. <https://doi.org/10.1016/j.ssi.2004.07.039>
- Hanif MB, Rauf S, Motola M et al (2021) Recent progress of perovskite-based electrolyte materials for solid oxide fuel cells and performance optimizing strategies for energy storage applications. *Mater Res Bull* 146:111612. <https://doi.org/10.1016/j.materresbull.2021.111612>
- Hao SJ, Wang C, Le LT et al (2017) Fabrication of nanoscale yttria stabilized zirconia for solid oxide fuel cell. *Int J Hydrogen Energy* 42:29949–29959. <https://doi.org/10.1016/j.ijhydene.2017.08.143>
- Hassen D, El-Safty SA, Tsuchiya K et al (2016a) Longitudinal hierarchy Co<sub>3</sub>O<sub>4</sub> mesocrystals with high-dense exposure facets and anisotropic interfaces for direct-ethanol fuel cells. *Sci Rep* 6:1–12. <https://doi.org/10.1038/srep24330>
- Hassen D, Shenashen MA, El-Safty SA et al (2016b) Nitrogen-doped carbon-embedded TiO<sub>2</sub> nanofibers as promising oxygen reduction reaction electrocatalysts. *J Power Sources* 330:292–303. <https://doi.org/10.1016/j.jpowsour.2016.08.140>
- He S, Zhang Q, Maurizio G et al (2018) In Situ Formation of Er<sub>0.4</sub>Bi<sub>1.6</sub>O<sub>3</sub> Protective layer at cobaltite cathode/Y<sub>2</sub>O<sub>3</sub>-ZrO<sub>2</sub> electrolyte interface under solid oxide fuel cell operation conditions. *ACS Appl Mater Interfaces* 10:40549–40559. <https://doi.org/10.1021/acsami.8b14026>
- He W, Wu X, Yang G et al (2017) BaCo<sub>0.7</sub>Fe<sub>0.22</sub>Y<sub>0.08</sub>O<sub>3-δ</sub> as an active oxygen reduction electrocatalyst for low-temperature solid oxide fuel cells below 600 °C. *ACS Energy Lett* 2:301–305. <https://doi.org/10.1021/acseenergylett.6b00617>
- Hibino T, Mizutani K, Yajima T, Iwahara H (1992) Evaluation of proton conductivity in SrCeO<sub>3</sub>, BaCeO<sub>3</sub>, CaZrO<sub>3</sub> and SrZrO<sub>3</sub> by temperature programmed desorption method. *Solid State Ion* 57:303–306. [https://doi.org/10.1016/0167-2738\(92\)90162-I](https://doi.org/10.1016/0167-2738(92)90162-I)
- Hou X, Zhao K, Marina OA et al (2019) NiMo-ceria-zirconia-based anode for solid oxide fuel cells operating on gasoline surrogate. *Appl Catal B Environ* 242:31–39. <https://doi.org/10.1016/j.apcatb.2018.09.095>
- Hou Y, Wang L, Bian L et al (2021) Excellent electrochemical performance of La<sub>0.3</sub>Sr<sub>0.7</sub>Fe<sub>0.9</sub>Ti<sub>0.1</sub>O<sub>3-δ</sub> as a symmetric electrode for solid oxide cells. *ACS Appl Mater Interfaces* 13:22381–22390. <https://doi.org/10.1021/acsami.1c02856>
- Hua B, Li M, Zhang YQ et al (2016) Facile synthesis of highly active and robust Ni-Mo bimetallic electrocatalyst for hydrocarbon oxidation in solid oxide fuel cells. *ACS Energy Lett* 1:225–230. <https://doi.org/10.1021/acseenergylett.6b00109>
- Huang C, Zhao G, Song Y et al (2022) Preparation of novel biodegradable cellulose nanocrystal proton exchange membranes for direct methanol fuel-cell applications. *ACS Sustain Chem Eng* 10:5559–5568. <https://doi.org/10.1021/acssuschemeng.2c00221>
- Huang H, Nakamura M, Su P et al (2007) High-performance ultrathin solid oxide fuel cells for low-temperature operation. *J Electrochem Soc* 154:B20. <https://doi.org/10.1149/1.2372592>
- Huang R, Antono E, Meredig B et al (2021) High-throughput characterization of Lu-doped zirconia. *Solid State Ion* 368:115698. <https://doi.org/10.1016/j.ssi.2021.115698>
- Hwang KJ, Jang M, Kim MK et al (2021) Effective buffer layer thickness of La-doped CeO<sub>2</sub> for high durability and performance on La<sub>0.9</sub>Sr<sub>0.1</sub>Ga<sub>0.8</sub>Mg<sub>0.2</sub>O<sub>3-δ</sub> electrolyte supported type solid oxide fuel cells. *J Eur Ceram Soc* 41:2674–2681. <https://doi.org/10.1016/j.jeurceramsoc.2020.11.036>
- Irshad M, Siraj K, Raza R, et al (2016) A brief description of high temperature solid oxide fuel cell's operation, materials, design, fabrication technologies and performance. *Appl Sci* 6. <https://doi.org/10.3390/app6030075>
- Ishihara T, Yan J, Shinagawa M, Matsumoto H (2006) Ni-Fe bimetallic anode as an active anode for intermediate temperature SOFC using LaGaO<sub>3</sub> based electrolyte film. *Electrochim Acta* 52:1645–1650. <https://doi.org/10.1016/j.electacta.2006.03.103>
- Istomin SY, Lyskov NV, Mazo GN, Antipov EV (2021) Electrode materials based on complex d-metal oxides for symmetrical solid oxide fuel cells. *Russ Chem Rev* 90:644–676. <https://doi.org/10.1070/rcr4979>
- Ito S, Mori T, Suzuki A et al (2019) Design of active site at heterointerface between brownmillerite type oxide promoter and fluorite cubic ZrO<sub>2</sub> in anode of intermediate temperature SOFCs. *ACS Appl Energy Mater* 2:5183–5197. <https://doi.org/10.1021/acsaem.9b00864>
- Iwahara H, Esaka T, Uchida H, Maeda N (1981) Proton conduction in sintered oxides and its application to steam electrolysis for hydrogen production. *Solid State Ion* 3–4:359–363. [https://doi.org/10.1016/0167-2738\(81\)90113-2](https://doi.org/10.1016/0167-2738(81)90113-2)
- Jamil A, Rafiq S, Iqbal T et al (2022) Current status and future perspectives of proton exchange membranes for hydrogen fuel cells. *Chemosphere* 303:135204. <https://doi.org/10.1016/j.chemosphere.2022.135204>
- Jang I, Lee H, Tamarany R et al (2020) Tailoring the ratio of a-site cations in Pr<sub>1-x</sub>Nd<sub>x</sub>BaCo<sub>1.6</sub>Fe<sub>0.4</sub>O<sub>5+δ</sub> to promote the higher oxygen reduction reaction activity for low-temperature solid oxide fuel cells. *Chem Mater* 32:3841–3849. <https://doi.org/10.1021/acs.chemmater.9b05378>
- Ji S, Cho GY, Yu W et al (2015) Plasma-enhanced atomic layer deposition of nanoscale yttria-stabilized zirconia electrolyte for solid oxide fuel cells with porous substrate. *ACS Appl Mater Interfaces* 7:2998–3002. <https://doi.org/10.1021/am508710s>
- Jiang N, Wachsman ED, Jung SH (2002) A higher conductivity Bi<sub>2</sub>O<sub>3</sub>-based electrolyte. *Solid State Ion* 150:347–353. [https://doi.org/10.1016/S0167-2738\(02\)00291-6](https://doi.org/10.1016/S0167-2738(02)00291-6)
- Joh DW, Park JH, Kim D et al (2017) Functionally graded bismuth oxide/zirconia bilayer electrolytes for high-performance intermediate-temperature solid oxide fuel cells (IT-SOFCs). *ACS Appl Mater Interfaces* 9:8443–8449. <https://doi.org/10.1021/acsami.6b16660>
- Kang H, Kim E, Jung SP (2017) Influence of flowrates to a reverse electro-dialysis (RED) stack on performance and electrochemistry of a microbial reverse electro-dialysis cell (MRC). *Int J Hydrogen Energy* 42:27685–27692. <https://doi.org/10.1016/j.ijhydene.2017.06.187>
- Kerman K, Ramanathan S (2014) Complex oxide nanomembranes for energy conversion and storage: a review. *J Mater Res* 29:320–337. <https://doi.org/10.1557/jmr.2013.301>

- Khan MZ, Mehran MT, Song RH et al (2018) A simplified approach to predict performance degradation of a solid oxide fuel cell anode. *J Power Sources* 391:94–105. <https://doi.org/10.1016/j.jpowsour.2018.04.080>
- Khan MZ, Song RH, Hussain A et al (2020) Effect of applied current density on the degradation behavior of anode-supported flat-tubular solid oxide fuel cells. *J Eur Ceram Soc* 40:1407–1417. <https://doi.org/10.1016/j.jeurceramsoc.2019.11.017>
- Kharton VV, Marques FMB, Atkinson A (2004) Transport properties of solid oxide electrolyte ceramics: a brief review. *Solid State Ion* 174:135–149. <https://doi.org/10.1016/j.ssi.2004.06.015>
- Kumar A, Jaiswal A, Sanbui M, Omar S (2016) Scandia stabilized zirconia-ceria solid electrolyte ( $x\text{Sc}1\text{CeSZ}$ ,  $5 < x < 11$ ) for IT-SOFCs: structure and conductivity studies. *Scr Mater* 121:10–13. <https://doi.org/10.1016/j.scriptamat.2016.04.023>
- Kumar A, Jaiswal A, Sanbui M, Omar S (2017) Oxygen-ion conduction in scandia-stabilized zirconia-ceria solid electrolyte ( $x\text{Sc}2\text{O}_3\text{-}1\text{CeO}_2\text{-(99-x)ZrO}_2$ ,  $5 \leq x \leq 11$ ). *J Am Ceram Soc* 100:659–668. <https://doi.org/10.1111/jace.14595>
- Kumar CNS, Bauri R, Reddy GS (2020) Phase stability and conductivity of rare earth co-doped nanocrystalline zirconia electrolytes for solid oxide fuel cells. *J Alloys Compd* 833:155100. <https://doi.org/10.1016/j.jallcom.2020.155100>
- Lee DS, Kim WS, Choi SH et al (2005) Characterization of  $\text{ZrO}_2$  co-doped with  $\text{Sc}_2\text{O}_3$  and  $\text{CeO}_2$  electrolyte for the application of intermediate temperature SOFCs. *Solid State Ion* 176:33–39. <https://doi.org/10.1016/j.ssi.2004.07.013>
- Lee JG, Park JH, Shul YG (2014) Tailoring gadolinium-doped ceria-based solid oxide fuel cells to achieve  $2\text{Wcm}^{-2}$  at  $550^\circ\text{C}$ . *Nat Commun* 5. <https://doi.org/10.1038/ncomms5045>
- Lee S, Zhang W, Khatkhatay F et al (2015) Ionic conductivity increased by two orders of magnitude in micrometer-thick vertical yttria-stabilized  $\text{ZrO}_2$  nanocomposite films. *Nano Lett* 15:7362–7369. <https://doi.org/10.1021/acs.nanolett.5b02726>
- Li M, Wang Y, Wang Y et al (2014) Bismuth doped lanthanum ferrite perovskites as novel cathodes for intermediate-temperature solid oxide fuel cells. *ACS Appl Mater Interfaces* 6:11286–11294. <https://doi.org/10.1021/am5017045>
- Li R, Yang J, Yan D et al (2021) Performance of  $\text{Al}_2\text{O}_3$  particle reinforced glass-based seals in planar solid oxide fuel cells. *Ceram Int* 47:7504–7510. <https://doi.org/10.1016/j.ceramint.2020.10.256>
- Liang YC, Chou YH (2020) Improved photoelectrode performance of chemical solution-derived  $\text{Bi}_2\text{O}_3$  crystals: via manipulation of crystal characterization. *RSC Adv* 10:45042–45058. <https://doi.org/10.1039/d0ra08746g>
- Lim HT, Virkar AV (2009) Measurement of oxygen chemical potential in  $\text{Gd}_2\text{O}_3$ -doped ceria- $\text{Y}_2\text{O}_3$ -stabilized zirconia bi-layer electrolyte, anode-supported solid oxide fuel cells. *J Power Sources* 192:267–278. <https://doi.org/10.1016/j.jpowsour.2009.03.035>
- Liu M, Ding D, Bai Y et al (2012) An efficient SOFC based on samaria-doped ceria (SDC) electrolyte. *J Electrochem Soc* 159:B661–B665. <https://doi.org/10.1149/2.032206jes>
- Liu T, Ren C, Fang S et al (2014) Microstructure tailoring of the nickel oxide-yttria-stabilized zirconia hollow fibers toward high-performance microtubular solid oxide fuel cells. *ACS Appl Mater Interfaces* 6:18853–18860. <https://doi.org/10.1021/am5046907>
- Lu Y, Cai Y, Souamy L et al (2018) Solid oxide fuel cell technology for sustainable development in China: an over-view. *Int J Hydrog Energy* 43:12870–12891. <https://doi.org/10.1016/j.ijhydene.2018.05.008>
- Lucia U (2014) Overview on fuel cells. *Renew Sustain Energy Rev* 30:164–169. <https://doi.org/10.1016/j.rser.2013.09.025>
- Lunca Popa P, S nderby S, Kerdsonpanya S et al (2017) Structural, morphological, and optical properties of  $\text{Bi}_2\text{O}_3$  thin films grown by reactive sputtering. *Thin Solid Films* 624:41–48. <https://doi.org/10.1016/j.tsf.2017.01.013>
- Ma G, Matsumoto H, Iwahara H (1999) Ionic conduction and nonstoichiometry in non-doped  $\text{Ba}_x\text{CeO}_{3-x}$ . *Solid State Ion* 122:237–247. [https://doi.org/10.1016/S0167-2738\(99\)00074-0](https://doi.org/10.1016/S0167-2738(99)00074-0)
- Mahato N, Banerjee A, Gupta A et al (2015) Progress in material selection for solid oxide fuel cell technology: a review. *Prog Mater Sci* 72:141–337. <https://doi.org/10.1016/j.pmatsci.2015.01.001>
- Malavasi L, Fisher CAJ, Islam MS (2010) Oxide-ion and proton conducting electrolyte materials for clean energy applications: structural and mechanistic features. *Chem Soc Rev* 39:4370–4387. <https://doi.org/10.1039/b915141a>
- Masciandaro S, Torrell M, Leone P, Taranc n A (2019) Three-dimensional printed yttria-stabilized zirconia self-supported electrolytes for solid oxide fuel cell applications. *J Eur Ceram Soc* 39:9–16. <https://doi.org/10.1016/j.jeurceramsoc.2017.11.033>
- Masina SM, Billing C, Erasmus RM, Billing DG (2021) Insights on the phase transitions, stability and conductivity in the  $\text{Bi}_2\text{O}_3\text{-WO}_3$  system. *J Electroceramics* 1. <https://doi.org/10.1007/s10832-021-00243-w>
- Matsuda M, Hosomi T, Murata K et al (2007) Fabrication of bilayered YSZ/SDC electrolyte film by electrophoretic deposition for reduced-temperature operating anode-supported SOFC. *J Power Sources* 165:102–107. <https://doi.org/10.1016/j.jpowsour.2006.11.087>
- Medvedev D, Murashkina A, Pikalova E et al (2014)  $\text{BaCeO}_3$ : Materials development, properties and application. *Prog Mater Sci* 60:72–129. <https://doi.org/10.1016/j.pmatsci.2013.08.001>
- Morales M, Pesce A, Slodczyk A et al (2018) Enhanced performance of gadolinia-doped ceria diffusion barrier layers fabricated by pulsed laser deposition for large-area solid oxide fuel cells. *ACS Appl Energy Mater* 1:1955–1964. <https://doi.org/10.1021/acsaem.8b00039>
- Morikawa H, Kikuchi H, Saito N (2009) Development and advances of a V-flow FC stack for FCX clarity. *SAE Tech Pap* 2:955–959. <https://doi.org/10.4271/2009-01-1010>
- Mu oz-Garc a AB, Ritzmann AM, Pavone M et al (2014) Oxygen transport in perovskite-type solid oxide fuel cell materials: insights from quantum mechanics. *Acc Chem Res* 47:3340–3348. <https://doi.org/10.1021/ar4003174>
- Ng CK, Ramesh S, Tan CY et al (2016) Microwave sintering of ceria-doped scandia stabilized zirconia as electrolyte for solid oxide fuel cell. *Int J Hydrog Energy* 41:14184–14190. <https://doi.org/10.1016/j.ijhydene.2016.06.146>
- Ng KH, Rahman HA, Somalu MR (2019) Review: enhancement of composite anode materials for low-temperature solid oxide fuels. *Int J Hydrog Energy* 44:30692–30704. <https://doi.org/10.1016/j.ijhydene.2018.11.137>
- Nie J, Zheng D, Ganesh KS et al (2021) Efficient strategy to boost the electrochemical performance of yttrium stabilized zirconia electrolyte solid oxide fuel cell for low-temperature applications. *Ceram Int* 47:3462–3472. <https://doi.org/10.1016/j.ceramint.2020.09.190>
- Nielsen J, Persson  H, Muhl TT, Brodersen K (2018) Towards high power density metal supported solid oxide fuel cell for mobile applications. *J Electrochem Soc* 165:F90–F96. <https://doi.org/10.1149/2.0741802jes>
- Nikonov AV, Kaygorodov AS, Kuterbekov KA, Bekmyrza KZ (2017) Microhardness and fracture toughness of  $\text{ZrO}_2\text{-Sc}_2\text{O}_3$  solid electrolyte, doped with rare-earth and transition metals. *Inorg Mater* 53:937–943. <https://doi.org/10.1134/S002016851709014X>
- Oh EO, Whang CM, Lee YR et al (2012) Extremely thin bilayer electrolyte for solid oxide fuel cells (SOFCs) fabricated by chemical

- solution deposition (CSD). *Adv Mater* 24:3373–3377. <https://doi.org/10.1002/adma.201200505>
- Omar S, Bin Najib W, Chen W, Bonanos N (2012) Electrical conductivity of 10 mol% Sc 2 O 3–1 mol% M 2 O 3– ZrO 2 ceramics. *J Am Ceram Soc* 95:1965–1972. <https://doi.org/10.1111/j.1551-2916.2012.05126.x>
- Omar S, Wachsman ED, Nino JC (2008) Higher conductivity Sm<sup>3+</sup> and Nd<sup>3+</sup> co-doped ceria-based electrolyte materials. *Solid State Ion* 178:1890–1897. <https://doi.org/10.1016/j.ssi.2007.12.069>
- Omar S, Wachsman ED, Nino JC (2006) A co-doping approach towards enhanced ionic conductivity in fluorite-based electrolytes. *Solid State Ion* 177:3199–3203. <https://doi.org/10.1016/j.ssi.2006.08.014>
- Orozco-Hernández G, Olaya-Flórez J, Pineda-Vargas C et al (2020) Structural, chemical and electrochemical studies of bismuth oxide thin films growth via unbalanced magnetron sputtering. *Surfaces and Interfaces* 21:100627. <https://doi.org/10.1016/j.surfin.2020.100627>
- Pan KJ, Hussain AM, Huang YL et al (2019) Evolution of solid oxide fuel cells via fast interfacial oxygen crossover. *ACS Appl Energy Mater* 2:4069–4074. <https://doi.org/10.1021/acs.aem.9b00185>
- Parbin A, Rafiuddin, (2022) The fabrication of a highly conductive ceria-embedded gadolinium-stabilized bismuth oxide nanocomposite solid electrolyte for low-temperature solid oxide fuel cells. *Mater Adv* 3:3316–3325. <https://doi.org/10.1039/d1ma01254a>
- Park CO, Akbar SA, Weppner W (2003) Ceramic electrolytes and electrochemical sensors. *J Mater Sci* 38:4639–4660. <https://doi.org/10.1023/A:1027454414224>
- Perry ML, Fuller TF (2002) A historical perspective of fuel cell technology in the 20th century. *J Electrochem Soc* 149:S59. <https://doi.org/10.1149/1.1488651>
- Politova TI, Irvine JTS (2004) Investigation of scandia-yttria-zirconia system as an electrolyte material for intermediate temperature fuel cells - influence of yttria content in system (Y<sub>2</sub>O<sub>3</sub>)<sub>x</sub>(Sc<sub>2</sub>O<sub>3</sub>)<sub>(11-x)</sub>(ZrO<sub>2</sub>)<sub>89</sub>. *Solid State Ion* 168:153–165. <https://doi.org/10.1016/j.ssi.2004.02.007>
- Price M, Dong J, Gu X et al (2005) Formation of YSZ-SDC solid solution in a nanocrystalline heterophase system and its effect on the electrical conductivity. *J Am Ceram Soc* 88:1812–1818. <https://doi.org/10.1111/j.1551-2916.2005.00389.x>
- Qian J, Zhu Z, Dang J et al (2013) Improved performance of solid oxide fuel cell with pulsed laser deposited thin film ceria-zirconia bilayer electrolytes on modified anode substrate. *Electrochim Acta* 92:243–247. <https://doi.org/10.1016/j.electacta.2013.01.017>
- Qiao J, Chen H, Wang Z et al (2020) Enhancing the catalytic activity of Y<sub>0.08</sub>Sc<sub>0.92</sub>TiO<sub>3</sub>-δAnodes through in Situ Cu exsolution for direct carbon solid oxide fuel cells. *Ind Eng Chem Res* 59:13105–13112. <https://doi.org/10.1021/acs.iecr.0c02203>
- Qiao Z, Xia C, Cai Y et al (2018) Electrochemical and electrical properties of doped CeO<sub>2</sub>-ZnO composite for low-temperature solid oxide fuel cell applications. *J Power Sources* 392:33–40. <https://doi.org/10.1016/j.jpowsour.2018.04.096>
- Rajendran S, Thangavel NK, Alkatie S et al (2021) Y, Gd, and Pr tri-doped perovskite-type proton conducting electrolytes with improved sinterability and chemical stability. *J Alloys Compd* 870:159431. <https://doi.org/10.1016/j.jallcom.2021.159431>
- Rashid NLRM, Samat AA, Jais AA et al (2019) Review on zirconate-cerate-based electrolytes for proton-conducting solid oxide fuel cell. *Ceram Int* 45:6605–6615. <https://doi.org/10.1016/j.ceramint.2019.01.045>
- Ren R, Wang Z, Meng X et al (2020a) Boosting the electrochemical performance of Fe-based layered double perovskite cathodes by Zn<sup>2+</sup> doping for solid oxide fuel cells. *ACS Appl Mater Interfaces* 12:23959–23967. <https://doi.org/10.1021/acsami.0c04605>
- Ren R, Wang Z, Meng X et al (2020b) Tailoring the oxygen vacancy to achieve fast intrinsic proton transport in a perovskite cathode for protonic ceramic fuel cells. *ACS Appl Energy Mater* 3:4914–4922. <https://doi.org/10.1021/acs.aem.0c00486>
- Riegraf M, Amaya-Dueñas DM, Sata N et al (2021) Performance and limitations of nickel-doped chromite anodes in electrolyte-supported solid oxide fuel cells. *Chemsuschem* 14:2401–2413. <https://doi.org/10.1002/cssc.202100330>
- Ruh R, Garrett HJ, Domagala RF, Patel VA (1977) The system zirconia-scandia. *J Am Ceram Soc* 60:399–403. <https://doi.org/10.1111/j.1551-2916.1977.tb15521.x>
- Sacanell J, Hernández Sánchez J, Rubio López AE et al (2017) Oxygen reduction mechanisms in nanostructured La<sub>0.8</sub>Sr<sub>0.2</sub>MnO<sub>3</sub> cathodes for solid oxide fuel cells. *J Phys Chem C* 121:6533–6539. <https://doi.org/10.1021/acs.jpcc.7b00627>
- Sandhu NK, Hanifi AR, Woldnik A et al (2016) Electrochemical performance of a short tubular solid oxide fuel cell stack at intermediate temperatures. *Appl Energy* 183:358–368. <https://doi.org/10.1016/j.apenergy.2016.08.179>
- Shah MAKY, Rauf S, Mushtaq N et al (2020) Semiconductor Fe-doped SrTiO<sub>3</sub>-δ perovskite electrolyte for low-temperature solid oxide fuel cell (LT-SOFC) operating below 520 °C. *Int J Hydrog Energy* 45:14470–14479. <https://doi.org/10.1016/j.ijhydene.2020.03.147>
- Shim JH, Chao CC, Huango H, Prinz FB (2007) Atomic layer deposition of yttria-stabilized zirconia for solid oxide fuel cells. *Chem Mater* 19:3850–3854. <https://doi.org/10.1021/cm070913t>
- Shimada H, Yamaguchi T, Sumi H et al (2017) Extremely fine structured cathode for solid oxide fuel cells using Sr-doped LaMnO<sub>3</sub> and Y<sub>2</sub>O<sub>3</sub>-stabilized ZrO<sub>2</sub> nano-composite powder synthesized by spray pyrolysis. *J Power Sources* 341:280–284. <https://doi.org/10.1016/j.jpowsour.2016.12.002>
- Shimada H, Yamaguchi T, Sumi H et al (2019) A key for achieving higher open-circuit voltage in protonic ceramic fuel cells: lowering interfacial electrode polarization. *ACS Appl Energy Mater* 2:587–597. <https://doi.org/10.1021/acs.aem.8b01617>
- Shin JS, Park H, Park K et al (2021) Activity of layered swedenborgite structured Y<sub>0.8</sub>Er<sub>0.2</sub>BaCo<sub>3</sub>.<sub>2</sub>Ga<sub>0.8</sub>O<sub>7+</sub>: δfor oxygen electrode reactions in at intermediate temperature reversible ceramic cells. *J Mater Chem A* 9:607–621. <https://doi.org/10.1039/d0ta11000k>
- Shin JW, Oh S, Lee S et al (2019) Ultrathin atomic layer-deposited CeO<sub>2</sub> overlayer for high-performance fuel cell electrodes. *ACS Appl Mater Interfaces* 11:46651–46657. <https://doi.org/10.1021/acsami.9b10572>
- Singh R, Chavan SB (2019) Processing and Properties of scandia-doped zirconia electrolyte for intermediate temperature SOFC. *ECS Trans* 7:2207–2212. <https://doi.org/10.1149/1.7279336>
- Smeacetto F, Salvo M, Ajitdoss LC et al (2010) Yttria-stabilized zirconia thin film electrolyte produced by RF sputtering for solid oxide fuel cell applications. *Mater Lett* 64:2450–2453. <https://doi.org/10.1016/j.matlet.2010.08.016>
- Son S, Koo B, Chai H et al (2021) Comparison of hydrogen production and system performance in a microbial electrolysis cell containing cathodes made of non-platinum catalysts and binders. *J Water Process Eng* 40:101844. <https://doi.org/10.1016/j.jwpe.2020.101844>
- Spirin A, Ivanov V, Nikonov A et al (2012) Scandia-stabilized zirconia doped with yttria: synthesis, properties, and ageing behavior. *Solid State Ion* 225:448–452. <https://doi.org/10.1016/j.ssi.2012.02.022>
- Steele BCH (2001) Material science and engineering: the enabling technology for the commercialisation of fuel cell systems. *J Mater Sci* 36:1053–1068. <https://doi.org/10.1023/A:1004853019349>
- Sudarsan P, Krishnamoorthy SB (2018) Grain boundary scavenging through reactive sintering of strontium and iron in samarium



- doped ceria electrolyte for ITSOFC applications. *Mater Res Bull* 100:446–457. <https://doi.org/10.1016/j.materresbull.2017.12.047>
- Sun W, Liu W (2012) A novel ceria-based solid oxide fuel cell free from internal short circuit. *J Power Sources* 217:114–119. <https://doi.org/10.1016/j.jpowsour.2012.05.065>
- Sun W, Shi Z, Qian J et al (2014) In-situ formed Ce<sub>0.8</sub>Sm<sub>0.2</sub>O<sub>2-δ</sub>-Ba(Ce, Zr)<sub>1-x</sub>(Sm, Y)<sub>x</sub>O<sub>3-δ</sub> core/shell electron-blocking layer towards Ce<sub>0.8</sub>Sm<sub>0.2</sub>O<sub>2-δ</sub>-based solid oxide fuel cells with high open cir. *Nano Energy* 8:305–311. <https://doi.org/10.1016/j.nanoen.2014.06.018>
- Sundmacher K (2010) Fuel cell engineering: toward the design of efficient electrochemical power plants. *Ind Eng Chem Res* 49:10159–10182. <https://doi.org/10.1021/ie100902t>
- Takahashi T, Esaka T, Iwahara H (1977) Conduction in Bi<sub>2</sub>O<sub>3</sub>-based oxide ion conductors under low oxygen pressure. I. Current blackening of the Bi<sub>2</sub>O<sub>3</sub>-Y<sub>2</sub>O<sub>3</sub> electrolyte. *J Appl Electrochem* 7:299–302. <https://doi.org/10.1007/BF01059169>
- Tran VHH, Kim E, Jung SP (2022) Anode biofilm maturation time, stable cell performance time, and time-course electrochemistry in a single-chamber microbial fuel cell with a brush-anode. *J Ind Eng Chem* 106:269–278. <https://doi.org/10.1016/j.jiec.2021.11.001>
- Virkar AV (1991) Theoretical analysis of solid oxide fuel cells with two-layer, composite electrolytes: electrolyte stability. *J Electrochem Soc* 138:1481–1487. <https://doi.org/10.1149/1.2085811>
- Vostakola MF, Horri BA (2021) Progress in material development for low-temperature solid oxide fuel cells: a review. *Energies* 14:1–55. <https://doi.org/10.3390/en14051280>
- Wang F, Lyu Y, Chu D et al (2019) The electrolyte materials for SOFCs of low-intermediate temperature: review. *Mater Sci Technol (United Kingdom)* 35:1551–1562. <https://doi.org/10.1080/02670836.2019.1639008>
- Wang Q, Fan H, Xiao Y, Zhang Y (2022) Applications and recent advances of rare earth in solid oxide fuel cells. *J Rare Earths*. <https://doi.org/10.1016/j.jre.2021.09.003>
- Wang Z, Cheng M, Bi Z et al (2005) Structure and impedance of ZrO<sub>2</sub> doped with Sc<sub>2</sub>O<sub>3</sub> and CeO<sub>2</sub>. *Mater Lett* 59:2579–2582. <https://doi.org/10.1016/j.matlet.2004.07.065>
- Wei B, Schroeder M, Martin M (2018) Surface cation segregation and chromium deposition on the double-perovskite oxide PrBaCo<sub>2</sub>O<sub>5+δ</sub>. *ACS Appl Mater Interfaces* 10:8621–8629. <https://doi.org/10.1021/acsami.7b17881>
- Wei CC, Li K (2008) Ytria-stabilized zirconia (YSZ)-based hollow fiber solid oxide fuel cells. *Ind Eng Chem Res* 47:1506–1512. <https://doi.org/10.1021/ie070960v>
- Wei L, Zhang J, Yu F et al (2019) A novel fabrication of yttria-stabilized-zirconia dense electrolyte for solid oxide fuel cells by 3D printing technique. *Int J Hydrogen Energy* 44:6182–6191. <https://doi.org/10.1016/j.ijhydene.2019.01.071>
- Wei T, Zhang LA, Chen Y et al (2017) Promising proton conductor for intermediate-temperature fuel cells: Li<sub>1.3</sub>9Sr<sub>0.1</sub>Zn(GeO<sub>4</sub>)<sub>4</sub>. *Chem Mater* 29:1490–1495. <https://doi.org/10.1021/acs.chemmater.6b03471>
- Wilberforce T, Alaswad A, Palumbo A et al (2016) Advances in stationary and portable fuel cell applications. *Int J Hydrogen Energy* 41:16509–16522. <https://doi.org/10.1016/j.ijhydene.2016.02.057>
- Williams KR (1994) Francis Thomas Bacon, 21 December 1904–24 May 1992. *Biogr Mem Fellows R Soc* 39:1–18. <https://doi.org/10.1098/rsbm.1994.0001>
- Xia C, Cai Y, Ma Y et al (2016) Natural mineral-based solid oxide fuel cell with heterogeneous nanocomposite derived from hematite and rare-earth minerals. *ACS Appl Mater Interfaces* 8:20748–20755. <https://doi.org/10.1021/acsami.6b05694>
- Xia C, Liu M (2001) Low-temperature SOFCs based on Gd<sub>0.1</sub>Ce<sub>0.9</sub>O<sub>1.95</sub> fabricated by dry pressing. *Solid State Ion* 144:249–255. [https://doi.org/10.1016/S0167-2738\(01\)00980-8](https://doi.org/10.1016/S0167-2738(01)00980-8)
- Xia C, Qiao Z, Shen L et al (2018) Semiconductor electrolyte for low-operating-temperature solid oxide fuel cell: Li-doped ZnO. *Int J Hydrog Energy* 43:12825–12834. <https://doi.org/10.1016/j.ijhydene.2018.04.121>
- Xu M, Yu J, Song Y et al (2020) Advances in Ceramic thin films fabricated by pulsed laser deposition for intermediate-temperature solid oxide fuel cells. *Energy Fuels* 34:10568–10582. <https://doi.org/10.1021/acs.energyfuels.0c02338>
- Yahiro H, Ohuchi T, Eguchi K, Arai H (1988) Electrical properties and microstructure in the system ceria-alkaline earth oxide. *J Mater Sci* 23:1036–1041. <https://doi.org/10.1007/BF01154008>
- Yamamoto O, Arati Y, Takeda Y et al (1995) Electrical conductivity of stabilized zirconia with ytterbia and scandia. *Solid State Ion* 79:137–142. [https://doi.org/10.1016/0167-2738\(95\)00044-7](https://doi.org/10.1016/0167-2738(95)00044-7)
- Yang G, Su C, Shi H et al (2020) Toward reducing the operation temperature of solid oxide fuel cells: our past 15 years of efforts in cathode development. *Energy Fuels* 34:15169–15194. <https://doi.org/10.1021/acs.energyfuels.0c01887>
- Yang J, Molouk AFS, Okanishi T et al (2015) Electrochemical and catalytic properties of Ni/BaCe<sub>0.75</sub>Y<sub>0.25</sub>O<sub>3-δ</sub> anode for direct ammonia-fueled solid oxide fuel cells. *ACS Appl Mater Interfaces* 7:7406–7412. <https://doi.org/10.1021/acsami.5b01048>
- Yasuda K, Uemura K, Shiota T (2012) Sintering and mechanical properties of gadolinium-doped ceria ceramics. *J Phys Conf Ser* 339:2–6. <https://doi.org/10.1088/1742-6596/339/1/012006>
- Yoshida T, Kojima K (2015) Toyota MIRAI fuel cell vehicle and progress toward a future hydrogen society. *Electrochem Soc Interface* 24:45–49. <https://doi.org/10.1149/2.F03152if>
- Zahid M, Savla N, Pandit S et al (2022) Microbial desalination cell: desalination through conserving energy. *Desalination* 521:115381. <https://doi.org/10.1016/j.desal.2021.115381>
- Zhang W, Wang H, Guan K et al (2019) La<sub>0.6</sub>Sr<sub>0.4</sub>Co<sub>0.2</sub>Fe<sub>0.8</sub>O<sub>3-δ</sub>/CeO<sub>2</sub> heterostructured composite nanofibers as a highly active and robust cathode catalyst for solid oxide fuel cells. *ACS Appl Mater Interfaces* 11:26830–26841. <https://doi.org/10.1021/acsami.9b06668>
- Zhang W, Wang H, Guan K et al (2020) Enhanced anode performance and coking resistance by in situ exsolved multiple-twinned Co-Fe nanoparticles for solid oxide fuel cells. *ACS Appl Mater Interfaces* 12:461–473. <https://doi.org/10.1021/acsami.9b14655>
- Zhang X, Robertson M, DeCes-Petit C et al (2007) Internal shorting and fuel loss of a low temperature solid oxide fuel cell with SDC electrolyte. *J Power Sources* 164:668–677. <https://doi.org/10.1016/j.jpowsour.2006.10.087>
- Zhang X, Robertson M, Yick S et al (2006) Sm<sub>0.5</sub>Sr<sub>0.5</sub>CoO<sub>3</sub> + Sm<sub>0.2</sub>Ce<sub>0.8</sub>O<sub>1.9</sub> composite cathode for cermet supported thin Sm<sub>0.2</sub>Ce<sub>0.8</sub>O<sub>1.9</sub> electrolyte SOFC operating below 600 °C. *J Power Sources* 160:1211–1216. <https://doi.org/10.1016/j.jpowsour.2006.03.035>
- Zhao J, Xu X, Zhou W et al (2017) Proton-conducting la-doped ceria-based internal reforming layer for direct methane solid oxide fuel cells. *ACS Appl Mater Interfaces* 9:33758–33765. <https://doi.org/10.1021/acsami.7b07938>
- Zhigachev AO, Rodaev VV, Zhigacheva DV et al (2021) Doping of scandia-stabilized zirconia electrolytes for intermediate-temperature solid oxide fuel cell: a review. *Ceram Int* 47:32490–32504. <https://doi.org/10.1016/j.ceramint.2021.08.285>
- Zhuyikov S (2000) An investigation of conductivity, microstructure and stability of HfO<sub>2</sub>-ZrO<sub>2</sub>-Y<sub>2</sub>O<sub>3</sub>-Al<sub>2</sub>O<sub>3</sub> electrolyte compositions for high-temperature oxygen measurement. *J Eur Ceram Soc* 20:967–976. [https://doi.org/10.1016/s0955-2219\(99\)00233-2](https://doi.org/10.1016/s0955-2219(99)00233-2)